Modelling the role of agriculture for the 20th century global terrestrial carbon balance

ALBERTE BONDEAU*, PASCALLE C. SMITH*[1], SÖNKE ZAEHLE*[1],
SIBYLL SCHAPHOFF*, WOLFGANG LUCHT*, WOLFGANG CRAMER*,
DIETER GERTEN*, HERMANN LOTZE-CAMPEN*, CHRISTOPH MÜLLER*§,
MARKUS REICHSTEIN*† and BENJAMIN SMITH‡

*Potsdam Institute for Climate Impact Research (PIK), Telegrafenberg, PO Box 601203, D-14412 Potsdam, Germany,
†Department of Forest Environment and Resources, DISAFRI, University of Tuscia, I-01100 Viterbo, Italy,
‡Department of Physical Geography and Ecosystems Analysis, Geobiosphere Science Centre, Lund University, S-223 62 Lund, Sweden,
§International Max Planck Research School on Earth System Modelling, Bundesstr. 53, 20146 Hamburg, Germany

Abstract

In order to better assess the role of agriculture within the global climate-vegetation system, we present a model of the managed planetary land surface, Lund–Potsdam–Jena managed Land (LPJmL), which simulates biophysical and biogeochemical processes as well as productivity and yield of the most important crops worldwide, using a concept of crop functional types (CFTs). Based on the LPJ-Dynamic Global Vegetation Model, LPJmL simulates the transient changes in carbon and water cycles due to land use, the specific phenology and seasonal CO_2 fluxes of agricultural-dominated areas, and the production of crops and grazing land. It uses 13 CFTs (11 arable crops and two managed grass types), with specific parameterizations of phenology connected to leaf area development. Carbon is allocated daily towards four carbon pools, one being the yield-bearing storage organs. Management (irrigation, treatment of residues, intercropping) can be considered in order to capture their effect on productivity, on soil organic carbon and on carbon extracted from the ecosystem. For transient simulations for the 20th century, a global historical land use data set was developed, providing the annual cover fraction of the 13 CFTs, rain-fed and/or irrigated, within $0.5°$ grid cells for the period 1901–2000, using published data on land use, crop distributions and irrigated areas. Several key results are compared with observations. The simulated spatial distribution of sowing dates for temperate cereals is comparable with the reported crop calendars. The simulated seasonal canopy development agrees better with satellite observations when actual cropland distribution is taken into account. Simulated yields for temperate cereals and maize compare well with FAO statistics. Monthly carbon fluxes measured at three agricultural sites also compare well with simulations. Global simulations indicate a $\sim$24% (respectively $\sim$10%) reduction in global vegetation (respectively soil) carbon due to agriculture, and 6–9 Pg C of yearly harvested biomass in the 1990s. In contrast to simulations of the potential natural vegetation showing the land biosphere to be an increasing carbon sink during the 20th century, LPJmL simulates a net carbon source until the 1970s (due to land use), and a small sink (mostly due to changing climate and CO_2) after 1970. This is comparable with earlier LPJ simulations using a more simple land use scheme, and within the uncertainty range of estimates in the 1980s and 1990s. The fluxes attributed to land use change compare well with Houghton's estimates on the land use related fluxes until the 1970s, but then they begin to diverge, probably due to the different rates of deforestation considered. The simulated impacts of agriculture on the global water cycle for the 1990s are $\sim$5% (respectively $\sim$20%) reduction in transpiration (respectively

Correspondence: Alberte Bondeau, tel. +49 331 288 2546,
fax +49 331 288 2600, e-mail: Alberte.Bondeau@pik-potsdam.de

Authorship after Lucht is alphabetical.

[1]Present address: Laboratoire des Sciences du Climat et de l'Environnement,
Orme des Merisiers, F-91191 Gif-sur-Yvette, France.

interception), and $\sim 44\%$ increase in evaporation. Global runoff, which includes a simple irrigation scheme, is practically not affected.

Introduction

Agriculture profoundly affects global carbon, water and nutrient cycles, as well as the planetary surface energy balance (Feddema *et al.*, 2005; Foley *et al.*, 2005). Accounting for croplands, pastures and rangelands, nearly 50% of the potentially vegetated land surface has been affected by agriculture (from Foley *et al.*, 2005). The global cropland area increased from $\sim 4 \times 10^6 \, \text{km}^2$ in 1700 to $\sim 18 \times 10^6 \, \text{km}^2$ in the 1990s, but $\sim 2 \times 10^6 \, \text{km}^2$ were abandoned in the same period of time (Ramankutty & Foley, 1999). Both clearing and abandonment of agricultural land use is continuing in many places. Earth system-wide feedbacks from this perturbation have been identified (e.g. Avissar & Werth, 2005; Gordon *et al.*, 2005), which may affect the stability of the climate system in the future – but they are at present incompletely quantified and may imply non-linear features in time or space.

Spatially explicit global parameterizations of land used for agriculture have been produced for the estimation of biophysical and biochemical features such as land surface albedo, energy balance, roughness, greenhouse gas (GHG) emissions, crop yields and carbon stocks. Differences in albedo and surface roughness between natural and cultivated vegetation alter atmospheric circulation, temperature and rainfall in coupled vegetation-climate modelling experiments (Xue, 1996; Bonan, 1999; de Noblet-Ducoudré *et al.*, 2000; Betts, 2001; Brovkin *et al.*, 2004, 2006). Global vegetation models running under historical or future climate scenarios generally show deforestation as generating enhanced carbon emission to the atmosphere, while regrowth is sequestering carbon (e.g. McGuire *et al.*, 2001; Brovkin *et al.*, 2004; Cramer *et al.*, 2004; Levy *et al.*, 2004). In these experiments, agricultural land use is usually described simply as harvest of a biomass fraction or as a replacement of forests by grasslands. Actual crops differ from grasslands, however, with respect to phenology and biogeochemical cycling. Land management (irrigation, fertilization, straw and residue processing, tillage/no tillage, etc.) alters the physical land surface and biogeochemical cycles, causing feedbacks to the climate (Boucher *et al.*, 2004; Lal, 2005; Ogle *et al.*, 2005). There are examples where land is managed purposefully towards atmospheric effects, in order to enhance carbon storage (Leahy *et al.*, 2004).

Planetary food production capacity has been estimated with global crop yield models (e.g. FAO, 1978;

Fischer *et al.*, 2002), which simulate the potential yield of major crops as a function of soil and climate. Actual yields are derived from potential ones through a 'management factor' based on FAO statistics. This method is used (e.g. by the integrated Earth system model IMAGE2, IMAGE team, 2001) to assess land use change in a context of climatic, demographic and socioeconomic change. In order to improve the representation of feedback mechanisms between crop biogeochemistry and climate, crop models with process-based representation of important biogeochemical cycles are now being used in several global assessments (e.g. EPIC, Tan & Shibasaki, 2003; or DayCent, Parton *et al.*, 1998; Stehfest *et al.* manuscript in preparation). Some large-scale crop models are being especially designed for this purpose (Challinor *et al.*, 2004, 2006).

In order to integrate agriculture into a comprehensive land biosphere model, Kucharik & Brye (2003) have added crop process modules to IBIS (Foley *et al.*, 1996), using algorithms from the EPIC crop growth model (Williams *et al.*, 1989). The resulting Agro-IBIS model simulates climate and management effects on biogeochemistry, as well as yields for maize and soybean in the United States (Donner & Kucharik, 2003; Kucharik, 2003). Gervois *et al.* (2004) have coupled the crop model STICS (Brisson *et al.*, 2003) to the land biosphere model ORCHIDEE (Krinner *et al.*, 2005). The resulting ORCHIDEE–STICS model improves the seasonal dynamics of the biophysical parameters of the land surface and biogeochemical cycles for wheat and maize in Western Europe (de Noblet-Ducoudré *et al.*, 2004).

These approaches share the property that they are either static (prescribed spatial properties of agriculture), are derived from computations of potential natural vegetation or grass (i.e., use a crop proxy), or link the separate modelling philosophy of crop production models into the respective land surface model. In contrast, we derive a biogeochemically consistent dynamic and flexible, parameter-scarce representation of global agriculture from the concept of plant functional types for inclusion in a Dynamic Global Vegetation Model (DGVM, Prentice *et al.*, 2006). DGVMs were initially developed to investigate the role of the terrestrial biosphere within the global carbon cycle, including climate feedbacks, considering potential rather than actual vegetation. They simulate the spatial and temporal dynamics of generic plant functional types (PFTs; tree/grass, evergreen/deciduous, broadleaf/evergreen,

etc.), as well as of important ecosystem functions (net primary production, heterotrophic respiration, evapotranspiration, runoff, etc.), making them suitable for broad-scale assessments in any biome (Cramer et al., 2001). Importantly, DGVMs allow the assessment of direct and indirect (climatic) effects of CO_2 enrichment on plant growth.

In addition to natural PFTs, we implement generic crop functional types (CFTs). CFTs are generalized and climatically adapted plant prototypes designed to capture the most widespread types of agricultural plant traits. Although they contain specific new functional formulations related to the development of yield-bearing organs, CFTs are directly compatible to PFTs for potential natural vegetation. Our approach permits the simulation of transient impacts of expanding (or declining) global agricultural areas on the terrestrial carbon and water cycles, here on the basis of the well-established Lund–Potsdam–Jena–DGVM (LPJ-DGVM; Sitch et al., 2003). Natural and agriculturally perturbed vegetation are simulated within the same biogeochemically consistent numerical framework. The annual land fractions occupied by different crops, natural or abandoned vegetation can be varied dynamically on the basis of land use. As we represent the global biosphere under human influence, we call this model version LPJmL ('LPJ managed Land'). The version presented here focuses on agricultural and grazing land only, without forest management.

The development of LPJmL serves two major purposes. First, it addresses nonlinear biophysical and biogeochemical features of continuing large-scale replacement of natural vegetation by agroecosystems, under CO_2 increase and climate change. Second, human societies worldwide make substantial economic and cultural use of ecosystem services (food, fibre and energy crops, but also climate regulation, water purification, etc.) – but the assessment of their future provision is still in an early stage (Alcamo et al., 2005). LPJmL is designed for the consistent quantification of multiple drivers (climate, CO_2, land management, land use change) on the future provision of these services.

In this paper, we describe and demonstrate LPJmL by investigating the impact of agriculture on the global carbon and water cycles in the 20th century, using historical climate and land use data, and by analysing present-day performance against selected benchmarking data.

Material and methods

A generic model for the world's arable and managed grassland ecosystems

A considerable range of simulation results from LPJ has been successfully compared with observations, such as the monitored seasonal cycle of atmospheric $[CO_2]$ (Sitch et al., 2003; Zaehle et al., 2005), the interannual variability in atmospheric $[CO_2]$ growth rate (Prentice et al., 2000; Peylin et al., 2005), the interannual variations in vegetation activity at high northern latitudes (Lucht et al., 2002), the runoff of major river catchments (Gerten et al., 2004b) and soil moisture (Wagner et al., 2003). This enhances our confidence in the representation of the coupled carbon and water cycles within LPJ for natural vegetation. We adapt LPJ to include those dynamics of croplands and grazing lands that are of relevance at the global to continental level.

As an alternative to the detailed parameterizations of agricultural crop cultivars used in crop production models (e.g. STICS, Brisson et al., 2003), which are difficult to apply on the global and century scales, we develop a 'CFT' concept, which is analogous and compatible to the 'PFT' concept used by LPJ and other biosphere models. Following, LPJmL can be used to estimate changes in basic stocks and fluxes of carbon and water, caused by land use, such as net primary productivity (NPP), net biome productivity (NBP), heterotrophic respiration (R_h) and evapotranspiration. In order to cover the major types of plants existing in agricultural ecosystems (arable crops and managed grasslands) worldwide, 13 CFTs were added, all sharing the fundamental biophysical and physiological functions of natural PFTs, but with additional specific agro-ecosystem-oriented functions and/or parameters (Table 1).

CFTs correspond to particular crops/grasses, or groups of crops with broadly similar functions. They do not mimic one specific cultivar of a crop, because this would limit the applicability of the model to only those sites where this cultivar exists, and because including all existing cultivars into the framework of a global model is impossible. To nevertheless account for variety-dependent plasticity, variety-specific crop characteristics (e.g. summer vs. winter cultivars, heat requirements) are determined internally to reflect the selection of an 'optimal' variety under the given local circumstances. Pastures and rangelands are represented by two basic grass CFTs, C_3- and C_4-managed grasses. In contrast to PFTs, a daily carbon allocation scheme is used for CFTs, in order to better capture the environmental and management influence on crop development and yield (see 'Crop development and growth').

Spatio-temporal arrangement of land cover types within a spatial unit

In agricultural landscapes, fields are separated from each other, usually containing a single crop only. LPJmL uses a number of distinct land segments: one natural

Table 1 Features/parameters of LPJmL for phenology and growth of CFTs

CFTs (other than managed grass)	Local adaptation: sowing date and cultivar parameters	Sowing date sdate (Julian day)	Base temperature Tb (°C)	Phenological heat units phu (°C day)	Vernalization needs pvd (days), trg (°C)	Maximal LAI LAI_{max}	Irrigation priority	Optimum* harvest index at harvest hi_{opt} (0–1)	Minimum[†] harvest index at harvest hi_{min} (0–1)
Temperate cereals (wheat, barley, rye, oat)	sdate, phu, pvd	f(temp) at 12 °C; st 5 °C; N:(270–60); S: (85–240); init: N: 330; S: 150	0	f(sdate) (1500–2500)	f(sdate) (0–60) (trg: 12 °C)	f(fert) (3–7)	8	0.4	0.2
Rice	double cropping in tropical Asia	First cycle fixed: N: 120; S: 200	10	single 1600 double 1500	No	5	1[‡]	0.5	0.25
Maize	sdate, Tb	f(temp, prec) st 14 °C; pp10 init: N: 140; S: 320	f(sdate) (5–15)	1600	No	f(fert) (3–7)	2	0.5	0.3
Tropical cereals (millet, sorghum)	sdate	f(prec) pp10 init: N: 150; S: 330	10	1500	No	2.5	7	0.25	0.01
Pulses (lentils)	No	Fixed N: 100; S: 280	3	2000	No	4	6	0.6	0.01
Temperate roots (sugar beet)	No	Fixed N: 90; S: 270	3	2700	No	5	5	2[§]	1.1[§]
Tropical roots (cassava)	sdate	f(prec) pp10 init: N:100; S: 280	20	2000	No	5	11	2[§]	1.1[§]
Sunflower	sdate, phu	f(temp) st 15 °C init: N:120; S: 300	6	f(sdate) (1000–1600)	No	3	4	0.3	0.2
Soybean	No	Fixed N: 140; S: 320	10	1000	No	3	3	0.3	0.01
Groundnuts	sdate	f(prec) pp10 init: N: 140; S: 320	14	1500	No	4	10	0.4	0.3
Rapeseed	sdate, phu, pvd	f(temp) at 17 °C; st 5 °C; N: (180–60); S: (0–240); init: N: 300; S: 120	0	f(sdate) (1700–2900)	f(sdate) (0–60) (trg: 12 °C)	4.5	9	0.3	0.15

$sdate$, sowing date (N, northern hemisphere; S, southern hemisphere); Tb, base temperature; phu, phenological heat units; pvd, vernalization requirements; trg, threshold temperature for vernalization; LAI_{max}, maximum LAI; hi_{opt}, harvest index optimum; hi_{min}, harvest index minimum; $temp$, temperature; $prec$, precipitation; $fert$, fertilization; init, initialization (default value). For sowing dates estimations based on temperature, f(temp), wt and st are the autumn (respectively spring) temperature thresholds considered for winter (respectively spring) types. For sowing date estimations based on precipitation, f(prec), pp10 is the total precipitation required during the last 10 days: 40 mm all around the world, 110 mm in tropical Asia. For maize, Tb is a function of the sowing date, f(sdate). For temperate cereals and maize, LAI_{max} is a function of the fertilizer use, f(fert). Init: initialization (default value). If not modified by LPJmL, values of Tb, LAI_{max}, hi_{opt}, hi_{min}, are taken from Neitsch et al. (2002).

Notes:
*No water stress;
[†]Severe drought conditions;
[‡]Rice is always irrigated;
[§]The harvest index is higher than 1 for belowground storage organs.
LPJmL, Lund–Potsdam–Jena managed Land; CFT, crop functional type.

segment, where LPJ is run without further modifications (natural PFTs and barren land coexist in a homogeneous mixture), and one to 26 (see 'Input data') managed segments, where LPJmL simulates the phenology and growth of each individual CFT. All fluxes and pools are updated independently for each segment, although all share the same macroclimate and soil texture for the grid cell. Management, such as irrigation, is applied for the appropriate segments only.

Land use change (prescribed from historical reconstructions or scenarios) affects the relative size of the segments in each grid cell on an annual time scale (Zaehle, 2005). Expanding agricultural land removes natural vegetation. Abandoned agricultural land is added to the natural segment and immediate recolonization occurs following the establishment rules in LPJ. The accounting of carbon in the biosphere in response to changing land use follows McGuire et al. (2001),

adapted by Zaehle et al. (2005): for agricultural expansion, the root biomass of the removed vegetation increases the litter pool, while the removed aboveground biomass is allocated to two carbon pools which are returned to the atmosphere with turnover times of 1 year (67%), and 25 years (33%). To simulate crop rotations, soil and litter carbon pools of new and existing agricultural land are mixed after harvest. For abandoned land, new vegetation is immediately mixed proportionally with the natural segment of the grid cell; soil and litter carbon pools are added to the corresponding pools. Figure 1 illustrates the fluxes between the different carbon pools.

Crop development and growth

All crops considered in LPJmL have annual life cycles or are harvested within 1 year, controlled by climate
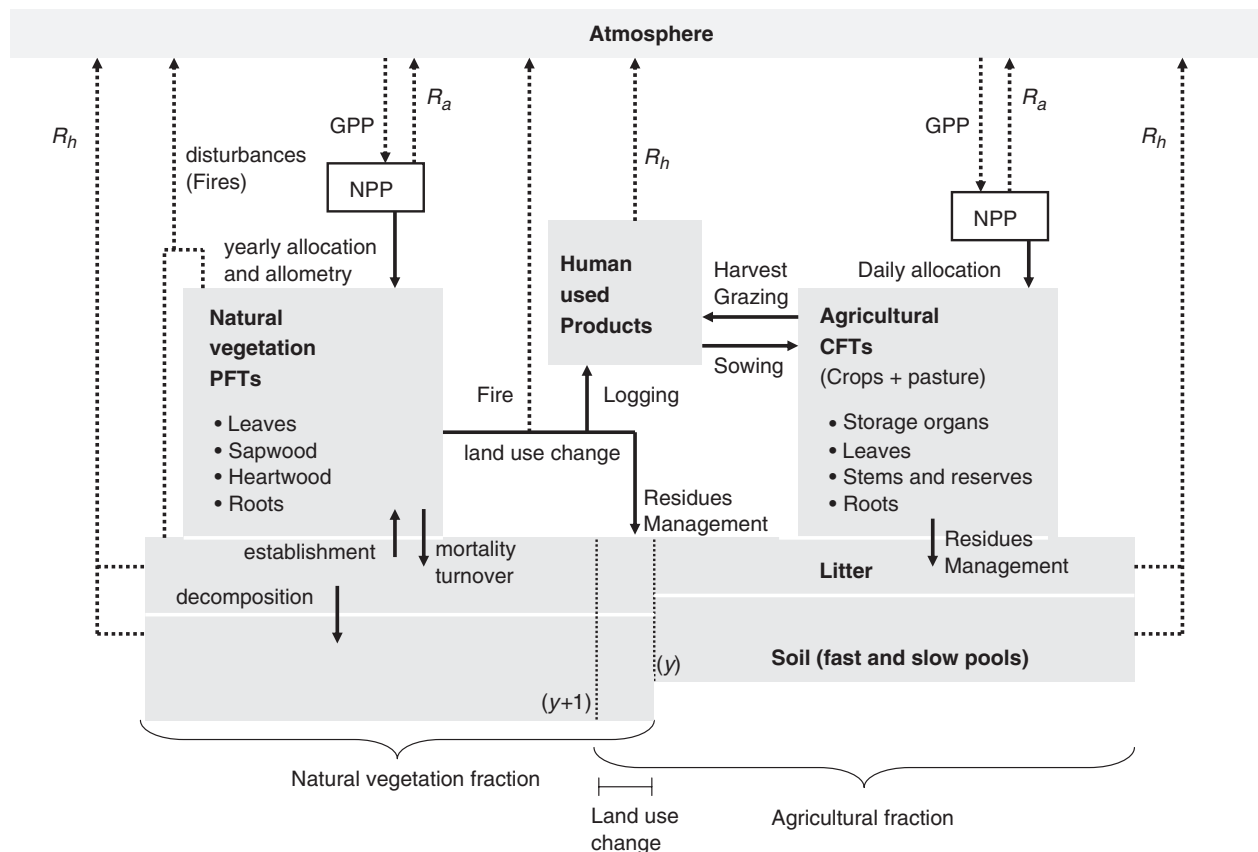
Fig. 1 Carbon pools and carbon fluxes simulated by Lund–Potsdam–Jena managed Land. Gross primary production (GPP), autotrophic respiration (R_a), net primary production (NPP) are computed separately for each plant functional type (PFT) and crop functional type (CFT). Carbon pools are vegetation (four different pools for natural vegetation and four for agriculture), litter, soil and human 'harvested' products. Natural vegetation and agriculture occupy distinct parts of the grid cell, yearly fractions are provided by land use. Product pools result from the regular human appropriation of organic material from agricultural areas, and eventually from land use change. The figure illustrates the case where a part of the natural fraction is converted to agriculture (see the limits at year y and at year $y + 1$), implying carbon emission (fires + logging) and changes in the amount of carbon of the litter and soil pools of the agricultural area. Dotted arrays represent CO_2 fluxes, continuous arrays organic material. R_h, heterotrophic respiration.

and human actions. In LPJ, growth is modelled using a combination of processes with daily time-steps (photosynthesis, respiration, evapotranspiration, applying a phenological scalar for seasonal variation), and processes with annual time-steps, in particular the allocation of photosynthates to various plant organs. Seasonal canopy development and the allocation of carbon to various organs in crops are crucial for yield, therefore, additional processes including daily allocation are taken into account for the CFTs. We base our implementation on concepts developed in the crop growth modelling of SWAT (Arnold et al., 1994), EPIC (Williams et al., 1989) and SWIM (Krysanova et al., 2000, 2005). The robust, process-based representation of the coupled CO_2 and H_2O exchanges in LPJ (Farquhar et al., 1980; Haxeltine & Prentice, 1996; Gerten et al., 2004b) is maintained in LPJmL. In contrast, many crop models reduce the potential crop-specific light-use efficiency due to environmental factors using empirical relationships (e.g. Stockle et al., 1992, for EPIC).

Sowing date. In agricultural management, the phenological cycle is initiated by planting or sowing (for simplicity referred to as 'sowing' in the remaining text), on a date chosen by the farmer under essentially pedo-climatic constraints. Most crops have climatic requirements which limit sowing date options to only a part of the year, (e.g. winter cereals with vernalization requirements; Harrison et al., 2000). We model sowing date deterministically as a function of climate, assuming rational decisions by farmers, based on their recent experience, for crops that are grown in a broad range of temperate and/or tropical latitudes (maize, sunflower), are known to range from winter to spring types (temperate cereals, rapeseed), or are managed according to water availability (groundnuts, tropical cereals, tropical roots). Parameters for temperature and/or rainfall dependencies are listed in Table 1. Besides providing a realistic spatial distribution of sowing dates, this allows to represent a key aspect of adaptation of crop management to climate change.

Sowing dates determined by temperature are modelled on the basis of the 20 previous years' average date on which mean daily temperature falls under ('winter' types) or rises over ('spring' types) a CFT-specific threshold value determined empirically (Table 1). Temperate cereals and rapeseed are winter types, or summer types if the winter is too long, (e.g. at northern latitudes). As a result, temperate cereals are sown in LPJmL from the beginning of October (most 'winter' types) to the end of April (late 'spring' types) in the northern hemisphere, with differing subsequent phenological developments. Sowing date determined by water availability is modelled on the basis of

the precipitation accumulated during the last 10 days (Table 1). For maize that grows in both temperate and tropical latitudes, temperature and/or precipitation thresholds are considered depending on latitude. Rice is assumed to grow twice per year in tropical Asia. Where no sowing-date climatic dependence could be established, a fixed sowing-date for each hemisphere is used (see fixed *sdate* in Table 1).

Phenology. Phenological development towards maturity is modelled using the heat unit theory (Boswell, 1926) by accumulating daily mean temperatures above a specific base temperature up to a maturity threshold. Instead of specific phenological phases (as in detailed crop models, e.g. Weir et al., 1984), we derive a phenological scalar increasing from 0 at sowing to 1 at maturity. We account for breeding or cultivar selection implicitly, assuming that the farmer will select the cultivar that is best adapted to the local pedo-climatic environment. For temperate cereals, rapeseed and sunflower, we determine the heat requirement, or phenological heat units (PHU), as a function of the sowing date, reflecting the length of the growing season. CFTs sown in relatively warm climate are modelled with higher heat requirements than in cooler climates. For temperate cereals or rapeseed, PHU is calculated from the fit of a quadratic curve to prescribed minimal and maximal PHU values that correspond to cultivars adapted to the coldest areas (earliest possible sowing date for winter crops or latest possible sowing date for spring crops) and to the warmest areas (winter sowing date). For sunflowers, PHU decreases linearly between a maximum value adapted to warm areas (early sowing date), and a minimum value adapted to cooler areas (late sowing date). The resulting variations of the PHU depending on the sowing date (i.e. on the climate) are shown in Fig. 2. For other CFTs, heat requirements are fixed, using standard values from the literature (Table 1). For temperate CFTs that benefit from winter dormancy (cereals and rapeseed), the vernalization requirement is also adjusted to the climate conditions (Table 1) and acts as a reduction factor on heat unit accumulation, slowing down progress on the phenological scale.

As for natural PFTs, the base temperature (T_b) for heat unit scheduling is the temperature value found to give the best linear fit of development rate to mean daily temperature. We use the values from SWAT (Neitsch et al., 2002) for all CFTs (Table 1), except for maize where a large base temperature range is allowed and determined from the sowing date (Fig. 3), permitting cultivar differences between tropical (T_b 15 °C) and temperate maize (T_b 5 °C for the northern areas in northern hemisphere, i.e. the latest sowing dates).
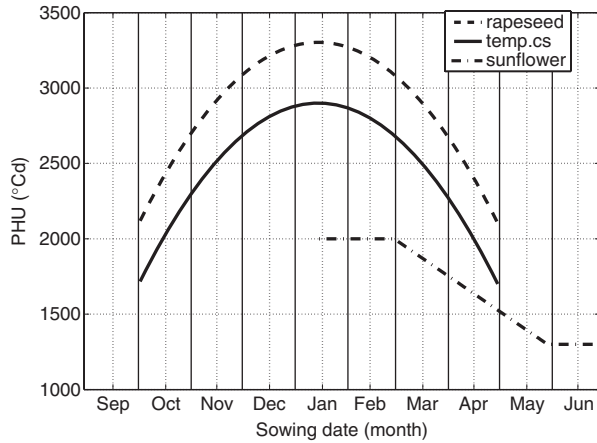
Fig. 2 The relationship between sowing date and heat requirements for three crop functional types. PHU, phenological heat units; °Cd, degrees-days; temp. cs, temperate cereals. Monthly values correspond to the Northern hemisphere (a shift of 6 months must be applied for the Southern hemisphere).
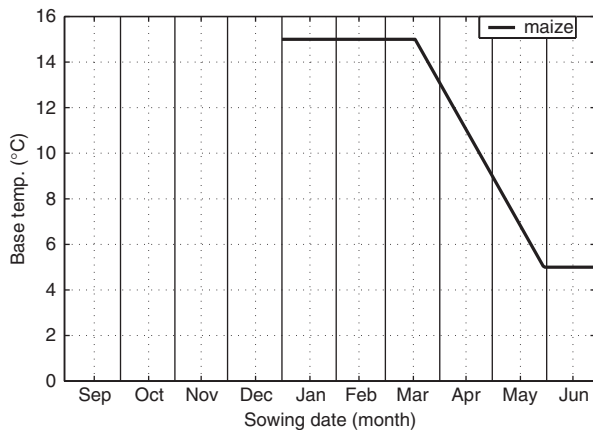
Fig. 3 Base temperature for heat requirement calculation in maize as function of sowing date.

Leaf area, growth and carbon allocation. CFTs in LPJmL use a daily carbon allocation scheme, rather than the year-end annual scheme used for PFTs (Sitch *et al.*, 2003), for several reasons. First, allocation of photosynthates to the different organs depends on the whole crop cycle, which can extend over 2 different years. Second, multiple cropping may occur through two cycles with different climate and/or management, leading to different maximum leaf area index (LAI) levels. Third, allocation to the yield-bearing organ occurs only during the final part of the development, depending on LAI development during the entire growth cycle.

The daily fraction of photosynthetically active radiation (fPAR) absorbed by the canopy is computed from daily LAI using Beer's law (Monsi & Saeki, 1953)

$$fPAR = 0.95(1 - e^{(k_l \times LAI)}), \qquad (1)$$

where k_l is the light extinction coefficient, fixed here to 0.5.

Assuming that 50% of the solar radiation is photosynthetically active (Monteith, 1972), we compute absorbed PAR (APAR) from fPAR which drives gross assimilation through photosynthesis and evapotranspiration assuming a 'big-leaf' approach. We constrain the shape of the LAI growth curve, by using sigmoid and quadratic functions to parameterize the LAI variations during the growth and senescent phases, as in SWAT (Fig. 4). The optimal leaf area development curve during the growth phase is expressed as

$$fLAI_{max} = \frac{fPHU}{fPHU + e^{(l_1 - l_2 \times fPHU)}}, \qquad (2)$$

where $fLAI_{max}$ is the fraction of the plant's maximum LAI corresponding to a given fraction of PHU, fPHU. l_1 and l_2 are two shape coefficients that are calculated from the fLAI and fPHU values at the first and second inflexion points on the leaf area development curve (see Table A4 of the SWAT User's Manual, Neitsch *et al.*, 2002). During the senescence phase, the LAI decrease of cereals, rapeseed and pulses follows the quadratic curve:

$$fLAI_{max} = \frac{(1 - fPHU)^2}{(1 - fPHU_{sen})^2}(1 - fLAI_{max\ harvest}) + fLAI_{max\ harvest}, \qquad (3)$$

while that of all other CFTs follows:

$$fLAI_{max} = \frac{\sqrt{1 - fPHU}}{\sqrt{1 - fPHU_{sen}}}(1 - fLAI_{max\ harvest}) + fLAI_{max\ harvest}, \qquad (4)$$
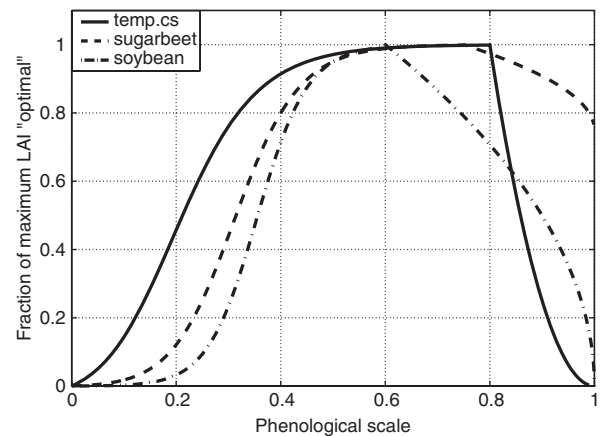
Fig. 4 Leaf area development for selected crop functional type as fraction of maximum leaf area index under optimal conditions (non water-stressed). temp. cs, temperate cereals.

where $fPHU_{sen}$ is the fraction of the growing season at which the senescence starts, and $fLAI_{max\ harvest}$ the fraction of crop maximal LAI still present at harvest. CFT-specific values are from SWAT (Neitsch *et al.*, 2002). Water stress reduces LAI growth directly, while temperature stress affects LAI growth through photosynthesis.

At sowing, photosynthesis in LPJmL starts on the basis of a small initial LAI supplied from seed reserves. The daily assimilation is allocated to four carbon pools: leaves, roots, harvestable storage organs (e.g. grains for cereals), and a pool representing stems and mobile reserves. The fraction of carbon assimilates entering each compartment is a function of heat unit accumulation (as in SWAT), adjusted for leaves and storage organs in case of water stress. At harvest, the biomass fraction of the storage organs is given by the harvest index (*hi*). The CFT-specific optimum and minimum (if water-stressed) *hi* are listed in Table 1. In case of water stress, leaf growth may not achieve the optimal LAI shape defined above, and the fraction of LAI_{max} reached at the peak of the canopy development will be lower than 1. On the other hand, leaf growth cannot exceed the value permitted by the LAI shape defined above, and extra assimilates are added to the unconstrained pool 'stems and mobile reserve'. Model runs for different CFTs under different environmental conditions show that the size of this unconstrained pool compares reasonably with the size of the other pools.

Maximum leaf area. A maximum LAI value, LAI_{max}, is prescribed for each CFT, which is reached under optimal climatic conditions. The values used in SWIM are generally higher than in SWAT, as SWIM is typically used for European intensive agriculture without nutrient limitations, where dense canopies are associated with high production. Using these values worldwide leads to overestimated yields in regions with more extensive management. Extensive management characterized by low fertilizer inputs leads generally to reduced canopy growth and lower LAI (Meireles *et al.*, 2002). As the model presently contains no explicit nutrient cycles, we proxy these processes by adapting the LAI_{max} value to the fertilizer use level for two dominant CFTs: temperate cereals and maize. We use values provided for the year 2000 at the country level from IFA (2002) to scale the LAI_{max} within the range given in Table 1: for countries with very low (respectively high) fertilizer application, the model uses the lowest (respectively highest) LAI_{max}. For rice, such a proxy is not directly applicable, because more information is required to characterize each of the two cycles within a year.

Irrigation. Irrigated segments are prescribed from land use data (see 'Input data'). When irrigation occurs, absence of water stress is assumed during the growing season. Additional water is provided as soon as the water content of the upper soil layer is insufficient to maintain a ratio between plant canopy water supply and atmospheric demand for transpiration of 0.7. The water balance routine determines the daily amount of irrigated water required to meet this condition. Owing to the additional water supply, evapotranspiration, as well as CO_2 uptake increase. Irrigation water is currently not depending on local water supply and is subtracted from runoff on an annual basis.

Harvest and residue management. Harvest occurs as soon as maturity is reached. At harvest, the storage organs are removed and their carbon content is assumed to respire within the same year. The carbon of the roots is added to the belowground litter pool. Different options can be considered for the management of crop residues, which depends on the regional agricultural system. Straw may either be burnt (Yadvinder-Singh *et al.*, 2004), grazed (Fernandez-Rivera *et al.*, 1989), processed for animal feed or bedding (Lopez-Guisa *et al.*, 1991; Powell *et al.*, 2004), or ploughed into the soil (Caviness *et al.*, 1986). This management may change due to new policies, (e.g. by encouraged removal of crop residues for the production of bioenergy in areas where previously they were more typically left on the fields; Sheehan *et al.*, 2004; Wilhelm *et al.*, 2004; Lal, 2005). Residues may also be incorporated into the soil in order to increase soil carbon sequestration or to reduce risks or emissions from fire (King *et al.*, 2004).

As there are no reliable global data for residue management practices, we here only compare two extreme options, 'residues in' where the crop straw/residues are left (and sent to the litter pool), and 'residues out' where they are removed almost entirely (90% of the aboveground biomass after yield harvest). In the latter case, the carbon content is respired to the atmosphere within the same year, without considering any carbon return from green manure or ash input. LPJmL does not simulate carbon emission due to different tillage practices.

Intercropping. In LPJmL, double-growing seasons within 1 year are at present allowed only for a monoculture system rice–rice. There is currently no representation of other multiple crops like the rice–wheat system widely found in South Asia (Fujisaka *et al.*, 1994), the wheat–soybean or maize–soybean practices in North America, or the use of nitrogen-fixing crops to enhance soil

fertility. Fallowing which is practiced for water conservation in some areas (e.g. the Great Plains in North America) is another form of management between crop cycles. After harvest of the main crop, LPJmL optionally allows extensive grass growth to simulate some form of intercropping growth. At the beginning of the new crop cycle, carbon from leaves and roots of this grass is added to the litter pool.

Managed grass/grazing. For the segment of the grid cell covered by 'managed grass', we prescribe a 'human' or 'livestock' disturbance. We do not distinguish between hay/ensilage production and grazing by animals (for simplicity, 'grazing' refers to both in the remainder of this paper). LAI development is driven by the daily carbon allocation to leaves, following the phenological scale. When LAI reaches a threshold, grazing occurs at high intensity, expressed as the removal of 50% of the aboveground biomass. This fraction, which contributes to animal metabolism, is modelled as a carbon flux to the atmosphere, except for a small part (5%, mostly faeces) that enters the litter pool. Livestock density is not yet considered.

Input data

Climate and atmospheric CO_2. Monthly data for mean temperature, precipitation, number of wet days, sunshine hours, gridded at $0.5°$ (longitude/latitude) resolution for 1901–2000, are based on CRU05 (New *et al.*, 2000; Österle *et al.*, 2003). A weather generator is used to determine the daily distribution of monthly precipitation (Gerten *et al.*, 2004b). Soil texture data and atmospheric CO_2 concentrations are used as in Sitch *et al.* (2003).

Land use. For the period 1901–2000, we have constructed a land use data set containing the percentage cover of each CFT, rain-fed and irrigated, within each grid cell, on a yearly time step. We use the cropland data set of Ramankutty & Foley (1999), which provides the historical cropland fraction of $0.5°$ grid cells until 1992. In order to extend this series to 2000, we simply assume the cropland fraction to remain constant after 1992. Leff *et al.* (2004) provide the distribution of 18 crops for 1990. A grazing grid-cell fraction is determined after comparison of the initial cropland fraction and the class 'grass and fodder' of the HYDE data set (Klein Goldewijk & Battjes, 1997) for 1970. By assuming no temporal change within the relative distribution of the different crops, we derive the annual distribution of the 13 CFTs for the entire period.

We use data on areas equipped for irrigation in 1995 (Döll & Siebert, 1999) to determine the irrigated agricultural fraction of the $0.5°$ grid cells, assuming irrigation to be efficient everywhere. In reality, some crops may only be irrigated during short periods in case of water scarcity or restriction, and irrigation efficiency differs widely across countries. In the absence of better information, we use these data as an approximation. We assume that, in 1901, only rice was irrigated. Then, the irrigated area of each grid cell increases linearly to its 1995 value, following the linear trend for global irrigation provided by Evans (1997). Only the segments of the grid cell covered by crops or managed grass may be irrigated. In order to estimate, which CFTs are most likely to be irrigated, we have established a priority list (derived mostly from European agricultural practices, see Table 1) and apply it globally. This rough approximation allows implementing both rain-fed and irrigated crops in LPJmL.

Simulation experiments

Global and grid-cell level simulations were performed with LPJmL and LPJ (where appropriate) to test essential model features (Table 2). A 900-year spin-up using the first 30 years of the climate and land use data sets is used to put carbon pools and fluxes in equilibrium. The impact of agriculture on the global carbon cycle during the 20th century was assessed in separate global simulation runs (Table 3). To illustrate the impact of management practices on the carbon cycle, we consider a range of four cases (residues removed or not, and intercropping permitted or not) for LPJmL and compare them with the original LPJ simulation.

Results

Comparison of model performance against observations

Sowing dates of temperate cereals. Figure 5 compares sowing dates for temperate cereals simulated by LPJmL to country-based crop statistics (USDA, 1994). For countries allowing this comparison, the north–south gradient of simulated sowing agrees well with observations. The simulated border between late summer types and early winter types occurs around $45°$ in the United States in agreement with the observations. In Western Europe, the simulated limit occurs further north than in North America because of a milder climate, as confirmed by the observations. However, LPJmL simulates summer cereals for Poland, where statistics report winter cereals. In most of Asia, simulations and observations agree well. For the winter types, the simulated sowing dates in the northern hemisphere show a large North–South range from October to December. This trend is confirmed in

Table 2 LPJmL simulations performed to test various model features

	Global/local run	CFT fraction cover used	Land use change considered	Period run	Variable analysed	Period analysed	Data used for comparison
(a) Sowing date	Global LPJmL	Yes	No	1971–2000 no spin-up	Annual *sdate*	[1990–1995] average	USDA crop calendar
(b) Phenology	Global LPJmL and LPJ	Yes	Yes	1901–2000 spin-up	Monthly fPAR	[1982–2000] average	Boston Univ. fPAR (NOAA/AVHRR)
(c) Yield estimation	Global LPJml	Yes	No	1971–2000 no spin-up	Harvested yield	[1991–2000] average	FAO national statistics
(d) C fluxes	Local LPJml	No (CFT prescribed)	No	1971–2001 no spin-up	Monthly GPP, R_{eco} and NEE	Individual years with eddy flux data	Eddy flux data
(e) Changes in carbon stocks/ fluxes due to agriculture and land use change for specific grid cells	Local LPJml and LPJ	Yes	Yes	1901–2000 spin-up	Soil and vegetation carbon, annual carbon fluxes (NPP, soil respiration, harvested carbon)	[1901–2000] trend	Qualitative assessment from literature

All simulations were made without intercropping, and with removal of residue. Intercropping affects fPAR (b), and all variables related to the carbon cycle (d) and (e). Residue management affects only the variables related to the carbon cycle (d) and (e). LPJ simulations are made in order to compare results for natural vegetation with those for actual vegetation.

LPJmL, Lund–Potsdam–Jena managed Land; fPAR, fraction of photosynthetically active radiation; CFT, crop functional type; NEE, net ecosystem exchange; GPP, gross primary production; *sdate*, sowing date; NPP, net primary production; R_{eco}, ecosystem respiration.

Europe by the data for several small countries located along that gradient, but cannot be tested in large countries such as the United States. In the southern hemisphere, simulated sowing dates (May) uniformly correspond to southern hemisphere winter types, as is also observed.

Satellite observations of monthly fPAR. The simulated seasonal fPAR of each grid cell is determined by the phenology of the different PFTs and CFTs that are present, and can be compared with satellite fPAR. Figure 6a shows the average seasonal fPAR for a large area in the Northern US and Canada Great Plains, a region characterized by rather homogenous climate and land use. Land use in these grid cells is at least 25% agricultural (cropland and grazing) and temperate cereals account for at least 25% of the agricultural fraction (37% on average). The satellite fPAR is compared with the modelled fPAR from, respectively, LPJ for natural vegetation, LPJ with natural grass growing in the agricultural areas (for comparison), and LPJmL. Natural vegetation in the region is simulated by LPJ as dominated by evergreen trees, therefore, its simulated fPAR is high during all months. When croplands are simulated as natural grasslands, the simulated fPAR reproduces the observed difference in the greenness activity of the canopy between summer and winter, but it represents higher activity in late summer than is observed. Simulated fPAR better approaches observations when crops are simulated by LPJmL: simulated fPAR is high only during a short period in July when the fields are covered by temperate cereals and rapeseed. Grassland, natural vegetation and some summer crops like maize explain why simulated fPAR remains around 0.4–0.5 until October. The satellite observations confirm the seasonal representation of fPAR at the regional level (including its mixture of natural vegetation, grassland and different crops) in LPJmL.

Figure 6b is an example of an agricultural system where simulated and observed seasonal fPAR agrees less well. In this area in semiarid Pakistan, only little grass grows naturally. Land use data indicate that the grid cell is nearly entirely cultivated (with 60% temperate cereals), and well irrigated. LPJmL simulates a single-crop cycle, in phase with the first fPAR cycle observed by the satellite. The satellite data show a second cycle, as important as the first one. This is probably explained by the double wheat–rice cropping, common in that area, but not modelled in LPJmL. Nevertheless, because of the irrigated crop cycle, LPJmL performs better than LPJ.

Generally, the phenology simulated by LPJmL agrees better with observations than the LPJ simulations not

Table 3 Global simulations for the period 1901–2000

20th century global runs	Land use data considered	Intercropping	Crop residue management	Period simulated	Period analysed
(a) LPJ	No	n/a	n/a	1901–2000 with spin-up	1901–2000 trend
(b) LPJmL	Yes	Yes	In	1901–2000 with spin-up	1901–2000 trend
(c) LPJmL	Yes	Yes	Out	1901–2000 with spin-up	1901–2000 trend
(d) LPJmL	Yes	No	In	1901–2000 with spin-up	1901–2000 trend
(e) LPJmL	Yes	No	Out	1901–2000 with spin-up	1901–2000 trend

LPJmL, Lund–Potsdam–Jena managed Land.
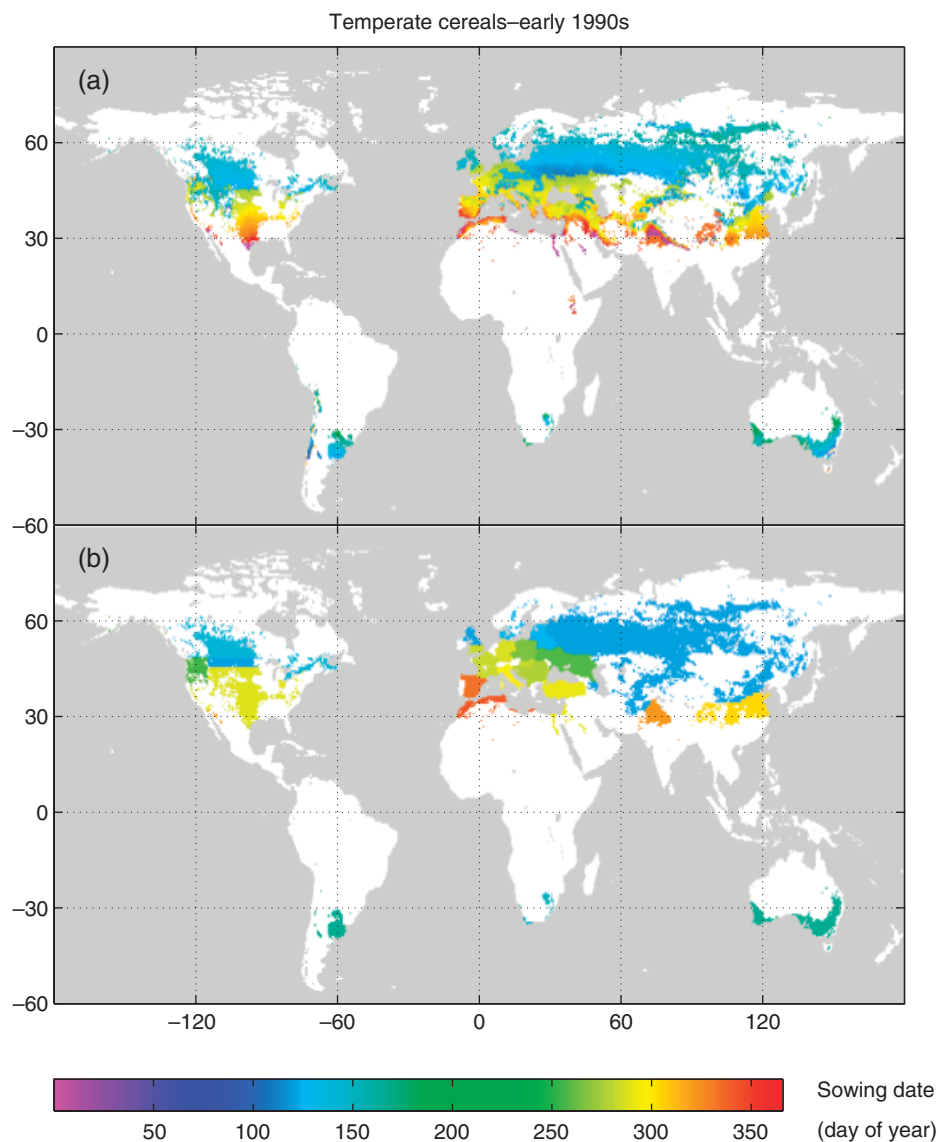
Fig. 5 Sowing dates for temperate cereals simulated with Lund–Potsdam–Jena managed Land (LPJmL); (a) and recorded by USDA (1994) statistics (b). Observed sowing dates are only shown for grid cells where land use data initiated LPJmL simulations for the respective crop. In countries with large climatic variation, only the central value of the reported range is shown (United States, Former Soviet Union, Mexico, Argentina, South Africa, Australia). Outside the areas of overlap Fig. 4b distinguishes winter and summer type sowing dates in the same country (United States, China, UK), otherwise only the dominant type is considered. Countries that are not reported by USDA are excluded.
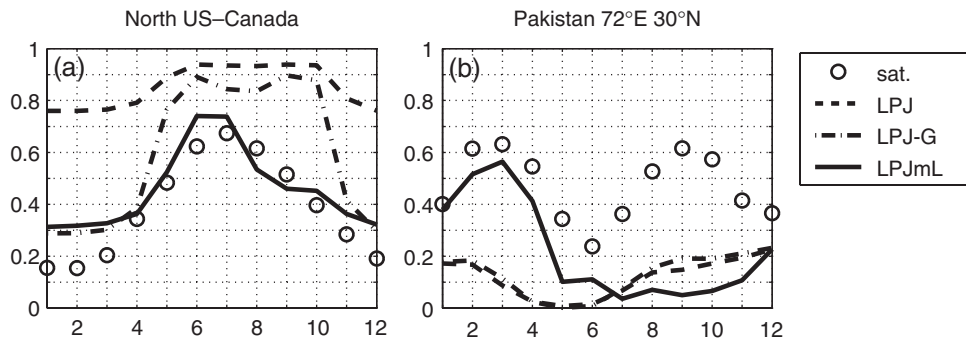
Fig. 6 Satellite-derived and simulated fraction of absorbed photosynthetically active radiation (fPAR) for a large area in the Northern United States and Canada (a, 767 grid cells, $1.6 \times 10^6 \, km^2$), and a dry area grid cell in Pakistan (b, 72°E, 30°N). Satellite data from the Boston University NOAA–AVHRR product Myneni *et al.* (1997), averaged over the period 1982–2000, interpolated to the 0.5° grid (sat.). Model simulations for Lund–Potsdam–Jena (LPJ) with natural vegetation, LPJ with natural grasslands occupying agricultural areas (LPJ-G), and with LPJ managed Land (LPJmL).
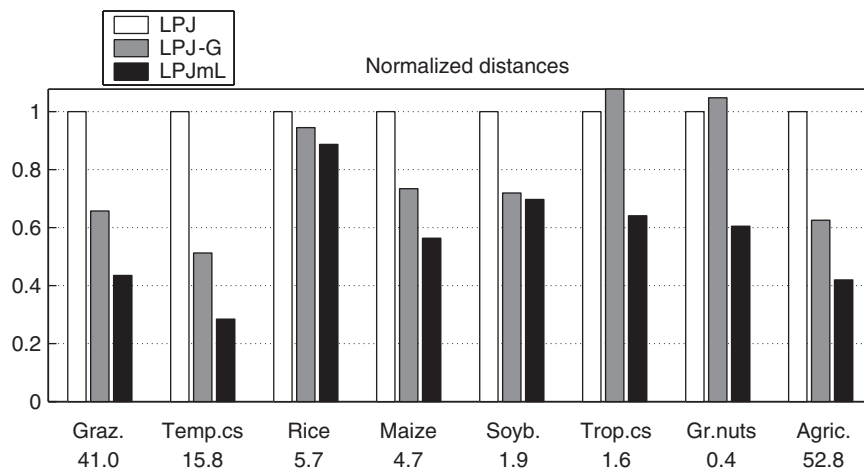
Fig. 7 Distances between monthly satellite observed fraction of photosynthetically active radiation (fPAR) and simulated fPAR (quadratic sum), for LPJ 'potential natural', LPJ 'grassland as cropland' (LPJ-G), and LPJ managed Land (LPJmL), normalized to that of LPJ 'potential natural'. Seven groups are considered [grid cells contain at least 25% agriculture, 25% of which is dominated by one crop functional type (CFT)], and the whole area with at least 25% agriculture. graz., grazing; temp.cs, temperate cereals; soyb., soybean; trop.cs, tropical cereals; gr.nuts, groundnuts; agric., agriculture. Area totals in $10^6 \, km^2$.

representing the agricultural seasonal cycles. We quantify this improvement by computing the sum of the 12 monthly squared distances between simulated and observed fPAR for CFT-specific dominated regions. Figure 7 shows the results for the seven CFTs where enough grid cells where available for the analysis, and for the total area of grid cells with at least 25% of agriculture coverage ($53 \times 10^6 \, km^2$, or a third of all land grid cells).

For all CFTs, simulated fPAR is closer to observed fPAR if LPJmL is used than otherwise. In most cases, using natural grassland as a surrogate for agriculture also improves the simulated fPAR of standard LPJ, but to a lesser degree. The performance of different CFTs varies, with the closest match observed for temperate cereals and the weakest for rice. This could be due to greater variability between the different rice varieties (and their respective crop calendar) grown in Asia, and mixtures with other crops. Modelling of the phenology for these subtropical agricultural systems needs to be improved. Overall, however, LPJmL clearly improves the simulated phenology of all pixels with at least 25% agricultural fraction.

Yield. FAO provides annual country yield statistics of major crops since 1961. In the long term, yield levels change mainly because of technological progress (plant breeding, fertilizer and pesticide use, etc.). We,

therefore, compare simulated and observed yields only for the period 1991–1995 and for two dominant CFTs worldwide; temperate cereals and maize. Rice is also important, but we have seen that the simulated phenology in rice areas is not well validated by the satellite fPAR. LPJmL needs to be improved before rice yields can be evaluated. Figures 8 and 10 show LPJmL-simulated yields for temperate cereals and maize (rain-fed only, and with irrigation). Figures 9 and 11 compare national totals for 45 (respectively 41) countries against FAO statistics. A number of yield-impacting processes are represented only in simplified form (fertilizer input) or not at all in LPJmL (pests and weeds), therefore only a first-order qualitative comparison can be made.

Temperate cereals. As expected, the highest yields are found in Western Europe, China, Japan, and Korea, due to favourable climatic conditions and high fertilizer inputs. Irrigation plays a particular role in some areas (the Nile valley and delta, northern Pakistan, Israel and Lebanon, and in some areas in Northern and Southern Africa, South America and Australia, cf. Fig. 8b).

On a country basis, the highest yields are simulated and observed in western Atlantic Europe, as confirmed by the FAO (Fig. 9). The lowest yields are simulated for countries under dry climate with limited irrigation and low fertilizers inputs, also in agreement with observations (Caucasus, Central Asia, Australia). However, under the more favourable climate of some former USSR countries, LPJmL simulates higher yields than reported. Large discrepancies are obtained for two countries with prescribed large irrigation (Egypt and Mexico). The rain-fed/irrigated ratio may be wrong in our input data.

Maize. Maize is the second CFT on the irrigation priority list (after rice, assumed to never encounter water stress). The rain-fed simulation, therefore, strongly differs from the one including irrigation (Fig. 10a and b). The high yields in the Mediterranean regions and in drier regions in the United States, India, China, Australia, southern Africa and southern America, clearly rely on irrigation. In the tropics, maize is grown extensively, and resulting yields are mostly low,
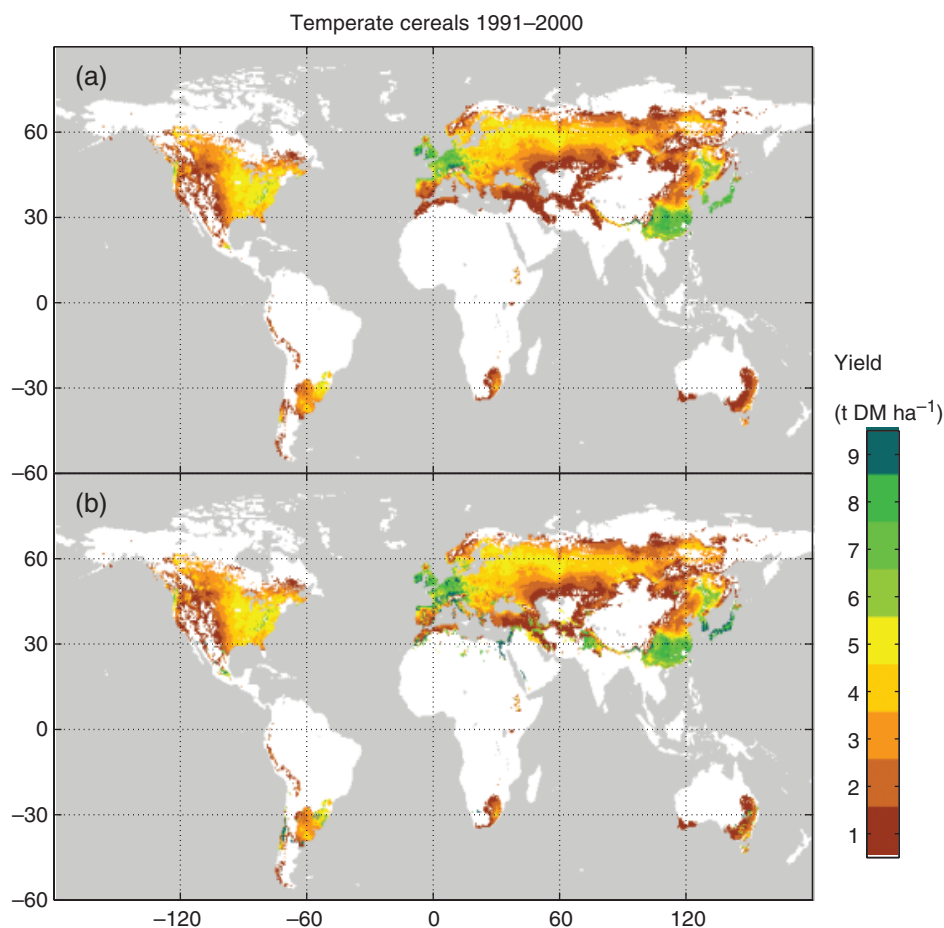
Fig. 8 Simulated yields for temperate cereals, averaged 1991–2000, rain-fed (a) and rain-fed plus irrigated (b).
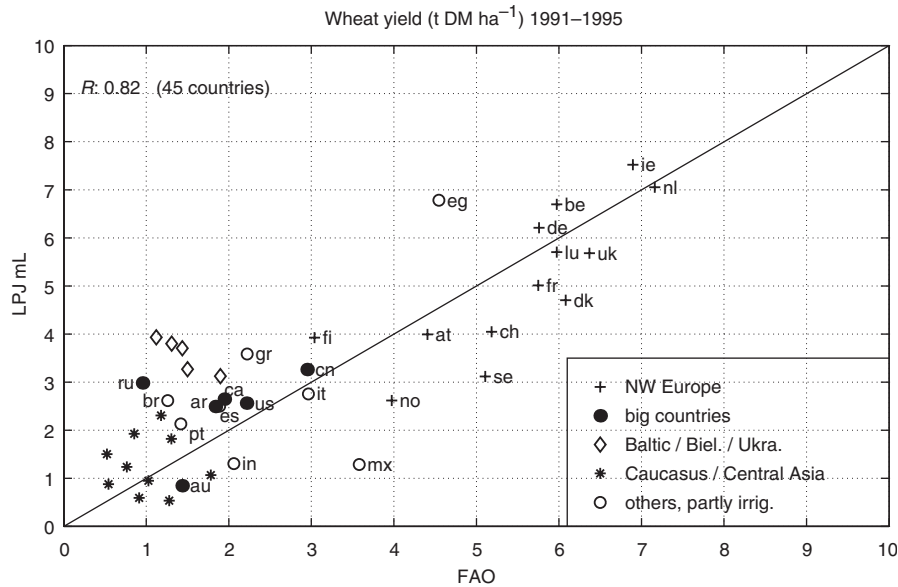
Fig. 9 Country-based comparison of simulated and observed yields for temperate cereals, based on FAO statistics. Internet country codes are used: ar, Argentina; at, Austria; au, Australia; be, Belgium; br, Brazil; ca, Canada; cg, Congo; ch, Switzerland; cn, China; de, Germany; dk, Denmark; eg, Egypt; es, Spain; fi, Finland; fr, France; gr, Greece; id, Indonesia; ie, Ireland; in, India; it, Italy; lu, Luxemburg; ml, Mali; mx, Mexico; ng, Nigeria; nl, the Netherlands; no, Norway; ph, Philippines; pt, Portugal; ru, Russian Federation; se, Sweden; th, Thailand; tr, Turkey; uk, United Kingdom; us, United States; ve, Venezuela; za, South Africa.

except for some highland areas in Cameroon, Eastern Africa, Colombia and Venezuela, where the relatively cool climate allows a longer cycle. LPJmL simulates the highest yields for temperate areas under intensive management, including irrigation if necessary (Western Europe, Mediterranean, China, Korea, some areas in the United States).

LPJmL generally overestimates yields for tropical countries, and underestimates yields for rather cold countries (Fig. 11). Simulations agree generally well with observations in countries with warm temperate climate and irrigation, with Greece having the highest yields (above 8 t DM ha^{-1}). Outliers are probably partly explained by inadequate quantification of irrigation (e.g. Portugal, South Africa, Georgia, Azerbaijan).

Seasonal CO$_2$ fluxes. Data from CO$_2$ flux measurements over crops were available for three sites (Fig. 12): Ponca and Bondville from the Ameriflux network (http://public.ornl.gov/ameriflux), and Jokioinen in Finland (Lohila *et al.*, 2004). Daily values for gross primary production (GPP) and ecosystem respiration (R_{eco}, sum of autotrophic and heterotrophic respiration) were provided from net ecosystem exchange data (NEE = R_{eco} − GPP) by the algorithm of Reichstein *et al.* (2005). As LPJmL is driven by monthly climatic data, we compare monthly simulated fluxes with monthly totals of observed fluxes. No local information regarding

sowing date and cultivar was used for the simulations, because we assume that the sites are typical for their respective regions and LPJmL is designed to represent the typical crop of the area. The same CFT (temperate cereals) is used to simulate winter wheat in Ponca and spring barley in Jokioinen.

LPJmL successfully reproduces the observed seasonal cycle for GPP, distinguishing the winter type in Ponca (early growth, maturity in June) from the spring type in Jokioinen (growth in late spring, mature in late summer). For Bondville, the phase of the seasonal cycle is also reproduced, both for soybeans and for maize. This is a notable agreement, as sowing dates are modelled rather than prescribed. The same holds true to some extent for R_{eco}.

At Bondville, simulated R_{eco} is much higher than the observations for both maize years 1997 and 1999. The low-observed R_{eco} values are explained by the fact that maize is grown in a maize/soybean rotation. As soybean produces much less biomass than maize, there is also less litter and root biomass, and soil respiration in the year following soybean is low. As there is no crop rotation in this LPJmL simulation, the soil respiration simulated at Bondville in 1997 or 1999 is based on a long-term simulation that grows maize each year, and generates therefore constantly high soil respiration. Despite the discrepancies for R_{eco}, the agreement between simulated and observed seasonal
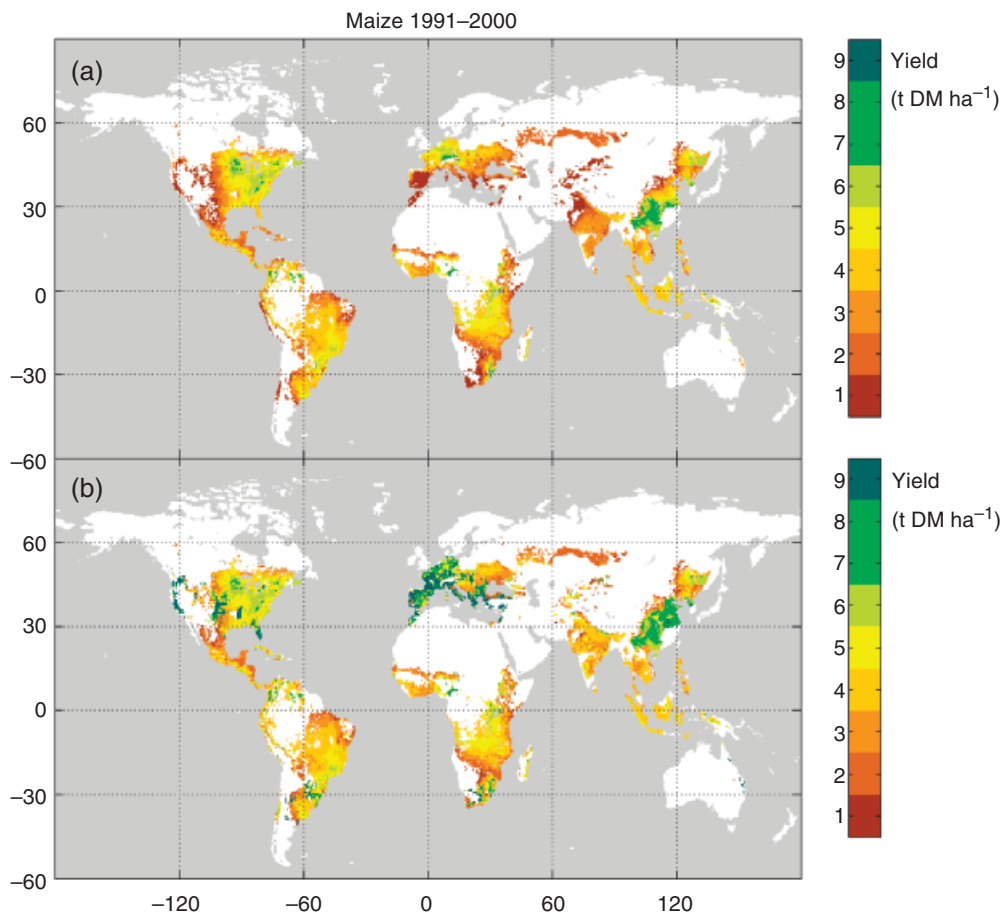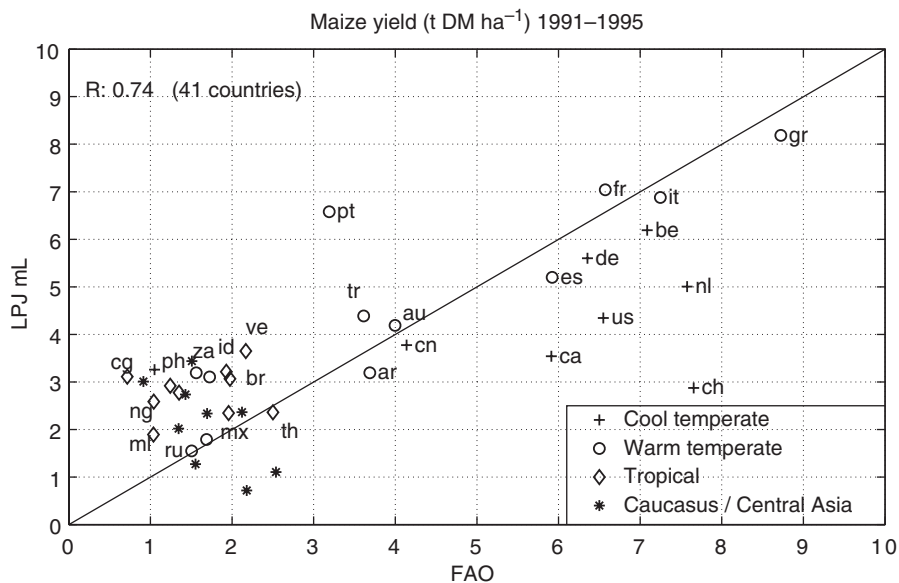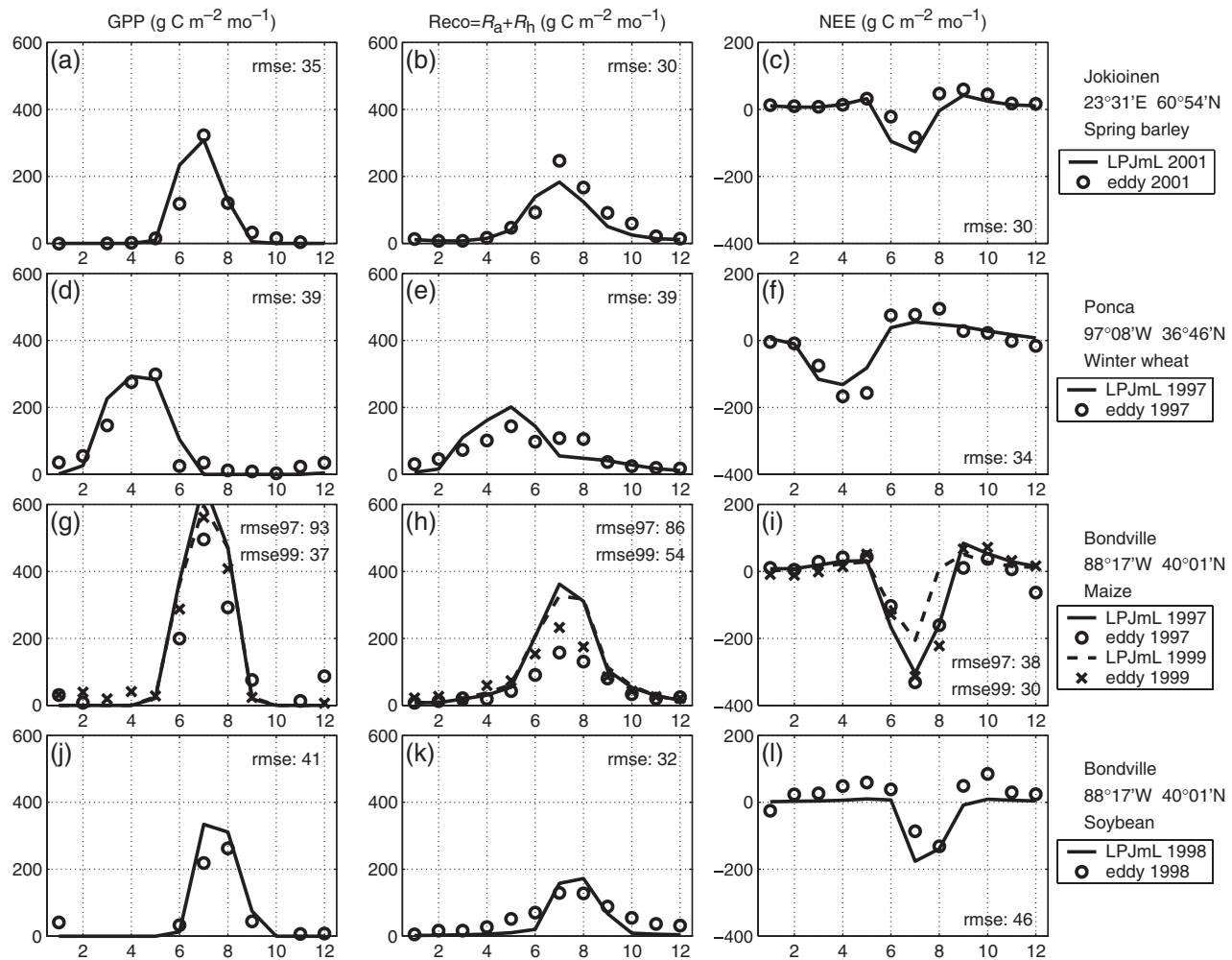
Fig. 10 Same as Fig. 8 for maize.

Fig. 11 Same as Fig. 9 for maize.

Fig. 12 Simulated and observed fluxes of carbon (in g C m^{-2} month^{-1}) for agricultural crops for three sites, Jokioinen (Finland, 23°31′E/60°54′N, 2001: spring barley), Ponca (Oklahoma, US, 97°08′W/36°46′N, 1997: winter wheat), and Bondville (IL, US, 88°17′W/40°00′N, 1997, 1999: maize, 1998: soybean). GPP, gross primary production, R_{eco}, ecosystem respiration (sum of autotrophic and heterotrophic respiration), and NEE, net ecosystem exchange.

NEE is rather good, although a good visual agreement (as for Bondville in 1997) can also be obtained when simulated GPP and R_{eco} are both too high (see rmse values on Fig. 12g–i).

Soil carbon content and carbon emission due to land use and land use change. We are unaware of any appropriate global data set for soil carbon content of agricultural soils. Different data sets refer to different soil depths. Past and present farming practices play an important role (tillage, residue management, crop rotation, etc.). We, therefore, do not attempt to test simulated soil carbon values under croplands or grazing land against literature data. Instead, we investigate the capability of LPJmL to reproduce the effect of land use and land use change on soil carbon content as reported in the literature (e.g. the meta analysis of Guo & Gifford,

2002). We evaluate model simulations for natural vegetation LPJ and LPJmL in seven selected grid cells with different climate, and different 20th century trends in agricultural land use (Fig. 13).

Generally, carbon pools (vegetation, soil) are considerably lower under cultivation, except for dry conditions, where the natural vegetation consists of grassland only (sites 4 and 5). NPP of croplands is similar to that of natural vegetation although is may be both higher (e.g. site 3) and lower (e.g. site 5). Interannual fluctuation of NPP, R_h and NBP are caused by climate variations.

For relatively stable land use, carbon pools and fluxes remain mostly constant, reacting only to changes in atmospheric [CO_2] and climate (e.g. sites 1 and 6).

With increasing agricultural land use, carbon pools decrease as natural forest is replaced by cropland (sites 2
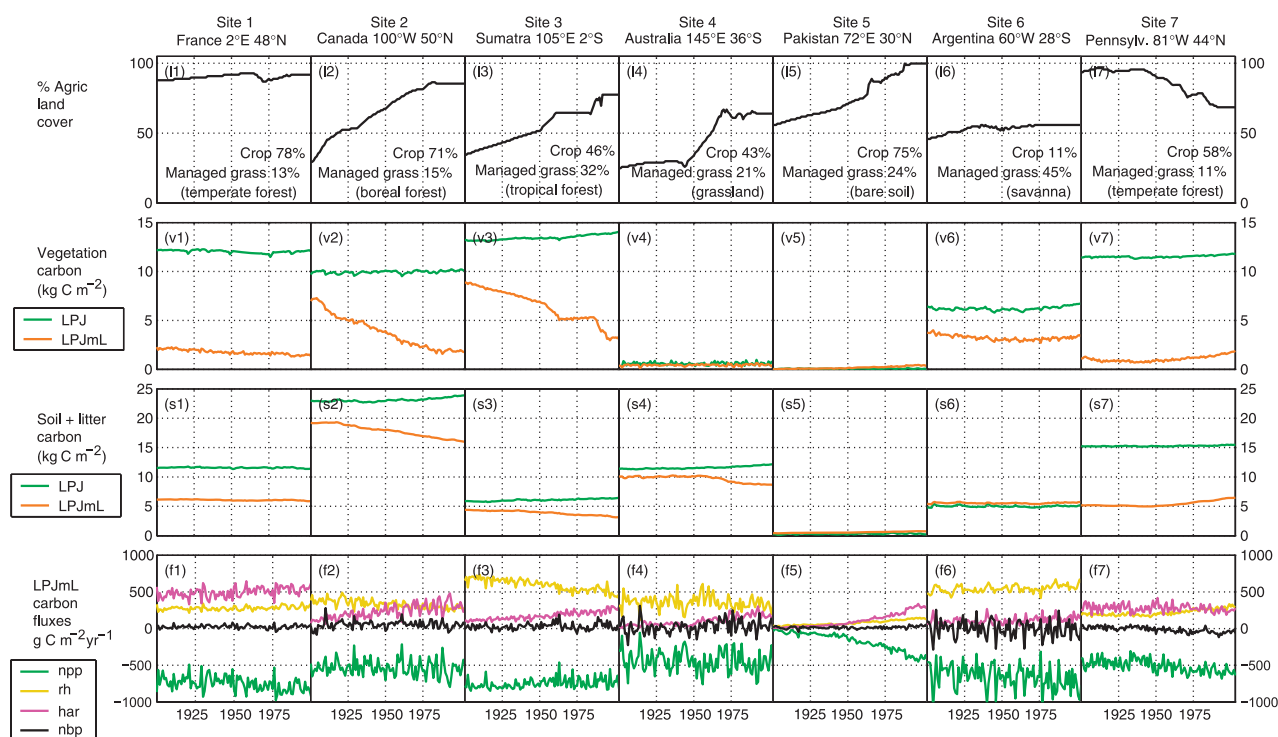
Fig. 13 Twentieth century trends in agricultural land use (percent, top row), vegetation carbon content [$kg\,C\,m^{-2}$, second row, Lund–Potsdam–Jena (LPJ) and LPJ managed Land (LPJmL)], soil and litter carbon content ($kg\,C\,m^{-2}$, third row, LPJ and LPJmL) and LPJmL carbon fluxes ($g\,C\,m^{-2}\,yr^{-1}$, bottom row, npp, net primary productivity; rh, heterotrophic respiration; har, harvest; and nbp, net biome productivity; i.e. the net carbon exchange or the sum of all fluxes), for seven selected grid cells representing different responses to land use change. Smaller order emissions from natural fires, or carbon sequestration through establishment or sowing are not shown. In the top row, the percents cover of crops and managed grassland at the end of the 20th century are given, and the biome characterization of the potential natural vegetation of the grid cell is indicated within brackets.

and 3). In natural grassland (site 4), vegetation carbon is unaffected by land use change but soil and litter carbon decline as additional carbon is removed by crop harvest. In semiarid regions (site 5), irrigation is responsible for the increased soil carbon. The increasing agricultural land use share results in increasing harvested carbon (f2–f5), and decreasing soil respiration following the decreases in soil carbon stocks.

In managed grasslands (site 6), soil carbon is higher than under natural vegetation (woody savanna), as parts of the vegetation carbon are regularly exported to the litter pool. This agrees with findings from Guo & Gifford (2002) on forest conversion to pasture in regions with this level of precipitation (annually ~ 350–$400\,mm$).

In the case of agricultural abandonment (site 7), carbon pools slowly start to build up, causing R_h to increase. However, the rate of the secondary forest growth seems to be underestimated.

With deforestation or afforestation, the net carbon balance (or NBP) tends to be either a small source or a small sink, respectively.

Overall, carbon fluxes and pools shown for these widely differing situations of land use and land use change correspond well to expectations and literature assessments, although many relevant processes are not represented in the model (e.g. top soil erosion).

Global simulations for the 20th century

The evaluation of LPJmL indicates that the model is robust enough to allow a mechanistic, process-based first-order assessment of the combined effects of land use change, climate change, atmospheric [CO_2] increase and changes in irrigation to be made at the global scale for the 20th century. The dominant factors influencing the magnitude of the agricultural perturbation of global biogeochemical cycles and climate are accounted for: (i) land use and land use changes (allocation of land to specific crops, deforestation, afforestation), (ii) influence of climate change and atmospheric [CO_2] increase on crop growth, (iii) irrigation increase. Significant management changes are not yet accounted for (plant

breeding, fertilizer and pesticides application, machinery), but the present model version can nevertheless be used to assess the impact of agriculture on carbon and water cycles. For the period 1901–2000, we have performed four global simulations at 0.5° resolution (with/without residue removal, with/without intercropping, Table 3).

Where cropland replaces natural forests, vegetation and soil carbon pools are reduced substantially (Fig. 14a and b). In some areas, however, irrigation allows agricultural areas to accumulate more vegetation carbon than natural vegetation would have done (Pakistan, Northern India, Egypt). In rangelands, LPJmL may simulate higher soil carbon contents than LPJ if pastures dominate the agricultural land cover (Central Africa, Australia, Argentina, Fig. 14b), but the difference is very small. The increase of NPP (Fig. 14c) is generally associated with irrigation and/or high fertilizer use. In some places (Southeast United States, Argentina), climate favours crops and pastures as simulated by LPJmL in terms of their productivity rather than the natural PFTs. In other areas, agricultural NPP decreases.

Total cropland area has increased during the first half of the century (Fig. 15a), most rapidly during the 1950s when several cropland extension programs were initiated worldwide (e.g. Central Asia). It then slowed down and reached quasi-stable conditions in the 1980s. During that period, deforestation in the tropics is largely compensated by afforestation in the temperate zones in the Ramankutty & Foley (1999) data set. Total vegetation carbon (Fig. 15b) for natural vegetation increased during the simulation due to CO_2 fertilization, while actual vegetation carbon (simulated by LPJmL) decreased when cropland areas increased most. However, when the cropland extension rate declined and the CO_2 effect became dominant, actual vegetation carbon content increased once more to reach approximately 520 GtC in the 1980s.

Management impacts are most visible for soil carbon (Fig. 15c): depending on residue management and on intercropping, the overall reduction in total soil carbon due to agriculture varies between 8% and 13%. As a large amount of carbon belongs to a pool with long turnover time, temporal changes are small.

The amount of harvested products increases during the 20th century (Fig. 15d and e) as a consequence of increasing agricultural area and productivity (Fig. 15f). LPJmL simulates the global crop harvest to be $\sim 2.2 \, \text{PgC yr}^{-1}$ in the 1990s, while grazing accounts for $\sim 3.6 \, \text{PgC yr}^{-1}$. Residue management has a strong impact on harvested carbon (Fig. 15e): between 6 and 9 PgC yr^{-1} are appropriated by humans in the 1990s.

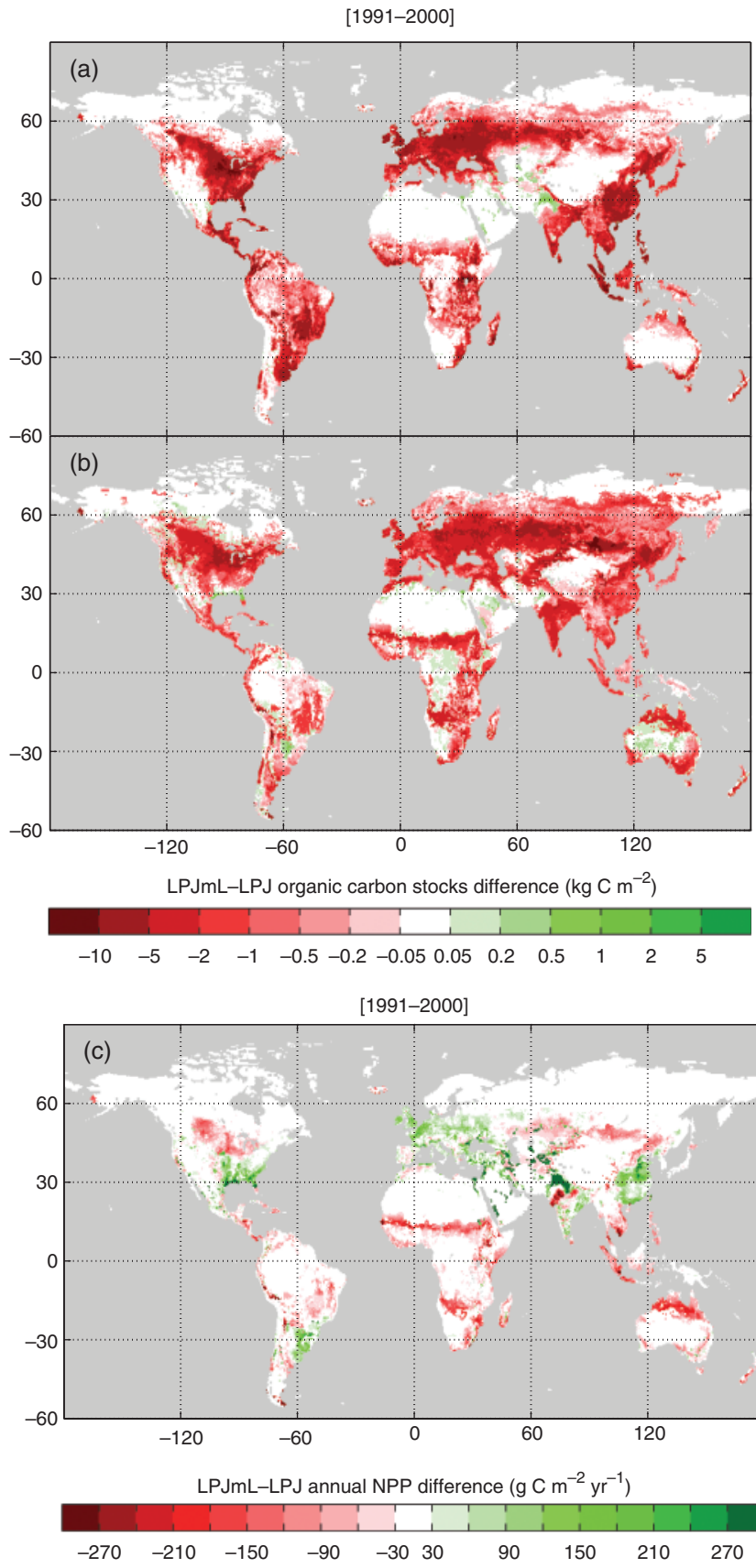Using the same model of CO_2 and water exchange, simulated NPP of actual and natural vegetation responds similarly to CO_2 fertilization and climate change during the 20th century (Fig. 15f). In the 1900s, LPJmL simulated a global actual NPP 10% lower than the potential NPP. This difference decreases with increasing irrigation.
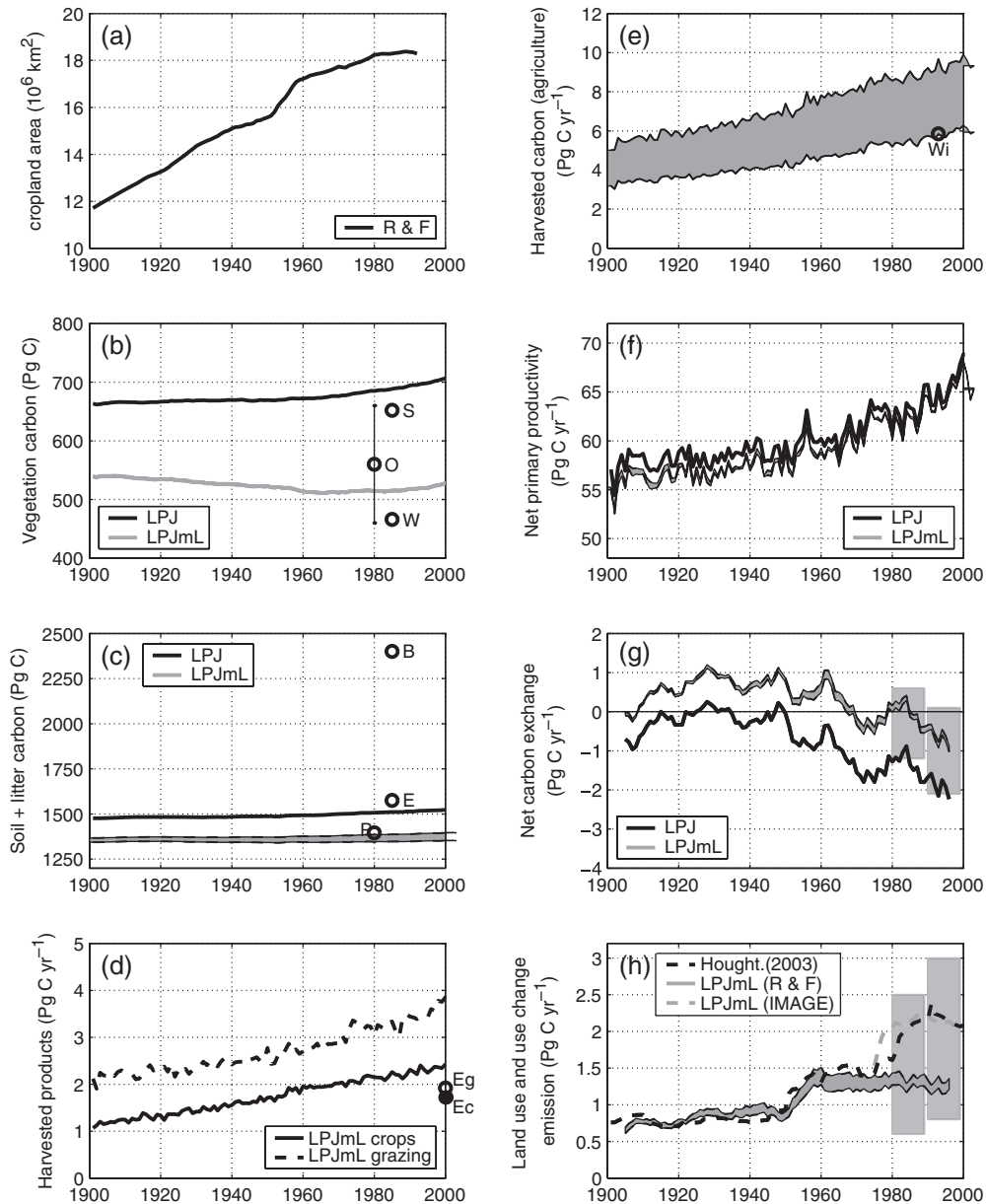
LPJ simulates a net sink of carbon in natural vegetation during the 20th century, especially in the second half (Fig. 15g). In contrast, LPJmL simulates the actual ecosystems to be a source until 1970, and then a small sink. This is due to emissions from land use change in the first half of the century, which are later compensated by CO_2 'fertilization'. In the 1980s LPJmL simulates the terrestrial biosphere to be nearly carbon neutral (slight source) with values between 0.04 and 0.16 PgC yr^{-1}, and in the 1990s a net sink occurs with values between −0.61 and –0.75 PgC yr^{-1}.

The difference between the net carbon fluxes simulated by LPJ and by LPJmL corresponds to the carbon emission due to land use and land use change (Fig. 15h) and can be compared with estimates made by Houghton (2003). Until the 1970s, LPJmL simulations follow the curve of Houghton (2003) quite closely. After 1980, croplands no longer increase in our land use data set while they do in the analysis of Houghton. Following Ramankutty & Foley (1999), deforestation is either reduced or compensated by afforestation that sequesters carbon. In consequence, the net biospheric carbon source remains lower than the Houghton's estimate. If LPJmL is run with the IMAGE land use data (IMAGE team, 2001), which display significant ongoing deforestation at the end of the 20th century, then the resulting land use emissions are much higher (grey dashed line in Fig. 15h), and closer to Houghton's estimate.

Owing to the tight coupling of transpiration and carbon uptake, changes in carbon fluxes due to agriculture are immediately associated with changes in water fluxes as simulated in LPJmL. Because of shorter seasonal cycles, global transpiration and interception are reduced when agriculture is simulated (Fig. 16a and b), while there is more evaporation (Fig. 16c). Intercropping (extensive grass) has only a secondary effect. In contrast, the impact on runoff is minimal (Fig. 16d). Using LPJmL without irrigation, Gerten et al. (2004a) showed that

Fig. 14 Difference in vegetation carbon (a), soil carbon (b), and net primary productivity (c) due to agriculture, averaged for the period 1991–2000, between a simulation for present day vegetation [Lund–Potsdam–Jena managed Land (LPJmL)] and a 'potential natural vegetation' simulation (LPJ).

[1991–2000]

LPJmL–LPJ organic carbon stocks difference (kg C m^{-2})

−10 −5 −2 −1 −0.5 −0.2 −0.05 0.05 0.2 0.5 1 2 5

[1991–2000]

LPJmL–LPJ annual NPP difference (g C m^{-2} yr^{-1})

−270 −210 −150 −90 −30 30 90 150 210 270

Fig. 15 Global agriculture-related carbon trends in the 20th century. The range of different Lund–Potsdam–Jena managed Land (LPJmL) results due to different management options (Table 3) is shown by filling the domain between the highest and the lowest individual LPJmL curves: (a) global cropland area (10^6 km²) from Ramankutty & Foley (1999); (b) vegetation carbon content (Pg C, LPJ and LPJmL), O, Olson et al. (1985); W, WBGU (1998); S, Saugier et al. (2001); (c) soil and litter carbon content (Pg C, LPJ and LPJmL), P, Post et al. (1982); E, Eswaran et al. (1993); B, Batjes (1996); (d) crops and grazing harvest (Pg C yr⁻¹, LPJmL), Ec, Erb and Kraussmann, (personal communication) for crops; Eg, idem for grazing; (e) total harvested carbon (Pg C yr⁻¹, LPJmL), Wi, Wirsenius (2003); (f) net primary productivity (Pg C yr⁻¹, LPJ and LPJmL); (g) net ecosystem exchange (Pg C yr⁻¹, LPJ and LPJmL), the grey-shaded regions represent the uncertainty range of different estimates based on analyses of CO_2 and O_2 budgets in the 1980s and 1990s (see 'Discussion'); (h) net flux between land biosphere and atmosphere due to land use and land use change (Pg C yr⁻¹), estimated by Houghton (2003), LPJmL with land use change from Ramankutty & Foley (1999), LPJmL with land use change from IMAGE (IMAGE team, 2001), the grey-shaded regions represent the uncertainty range of different estimates provided by Schimel et al. (2001) for the 1980s and for the 1990s, and House et al. (2003) for the 1990s.

agriculture slightly increases runoff. This very small difference is visible at the beginning of our simulation, but as irrigation increases during the 20th century, more water is taken out from the rivers and transpired by plants. As a result, at the end of the 20th century actual runoff is no longer higher than natural runoff.
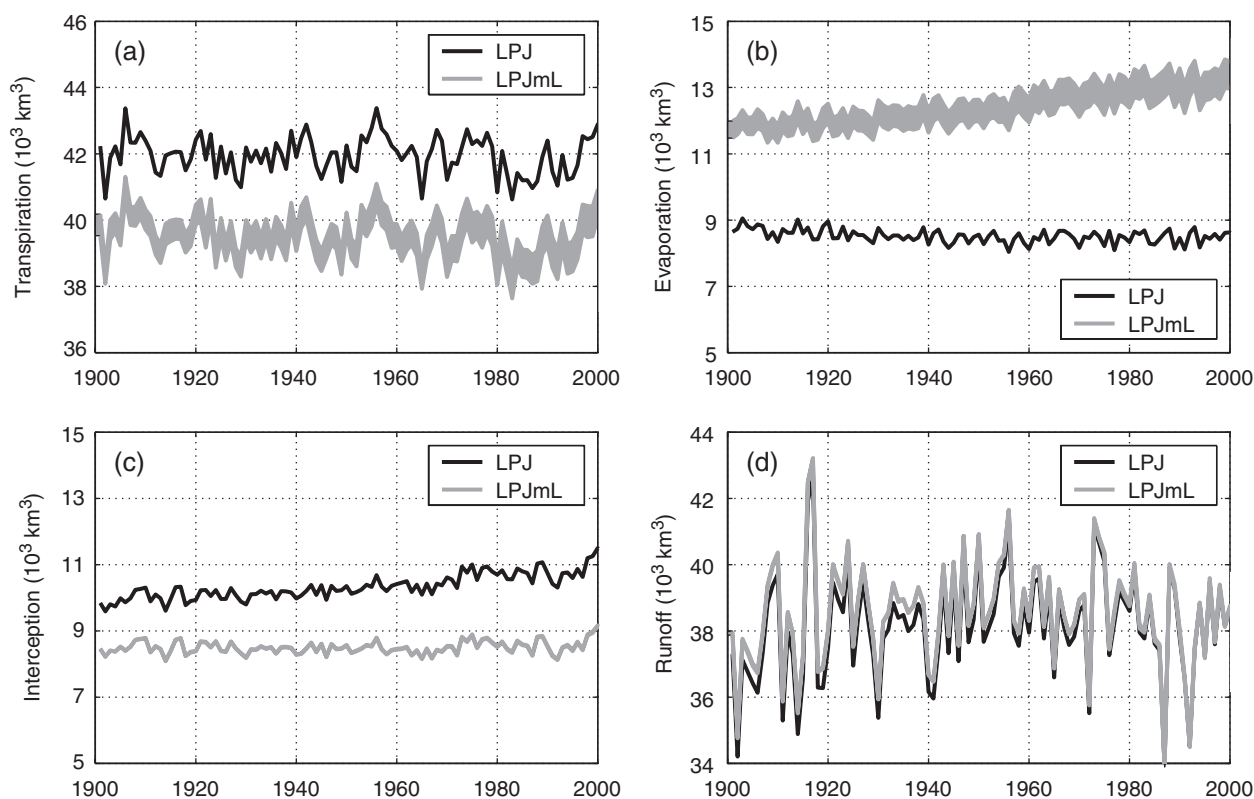
Fig. 16 Global agriculture-related water trends in the 20th century: (a) transpiration [10^3 km^3, Lund–Potsdam–Jena (LPJ) and LPJ managed Land (LPJmL)]; (b) interception (10^3 km^3, LPJ and LPJmL); (c) evaporation (10^3 km^3, LPJ and LPJmL); (d) runoff (10^3 km^3, LPJ and LPJmL).

Discussion

LPJmL is a functional representation of the world's terrestrial ecosystems combining natural vegetation, agricultural crops and grazing land. The model is capable of assessing the physical and biogeochemical responses of the land biosphere to changes in land use, climate and atmospheric CO_2, including the yields of major crops under given conditions of agrotechnological development. In this section, we compare our global results with published estimates. We also address remaining shortcomings of the approach and we indicate steps towards further improvements.

NPP of agricultural areas

Using satellite data and a light use efficiency (LUE) model, DeFries et al. (1999) provide a map of changes in NPP due to land use for the late 1980s. These results are sensitive to the LUE parameterization, but it is informative to compare them with LPJmL. Agreement is good in many areas (Fig. 14c): agriculture increases NPP in intensively managed or irrigated areas (Europe, China, Pakistan, Argentina, southern United States), and de-

creases it elsewhere. But as temperate cereals and maize are indicated to be grown extensively in United States and Australia (IFA, 2002), we find reduced NPP both in the US Central Plains and in the Australian wheat belt. This is in contrast with both, regional studies demonstrating high intensity in these regions (e.g. Bradford et al., 2005), resulting in an increase of agricultural NPP compared with natural NPP, and also with the satellite-driven LUE model (DeFries et al., 1999). LPJmL cannot reproduce these features as long as no management data are available at the regional scale.

Global carbon pools

The simulated global biomass of the actual vegetation (520 Gt C in the 1980s) is on the same order as published estimates: 560 ± 100 Gt C (Olson et al., 1985), 466 Gt C (WBGU, 1998), 652 Gt C (Saugier et al., 2001). Global estimates of soil carbon remain uncertain and vary strongly in the literature. Values of 1395 and 1576 Gt C are provided by Post et al. (1982) and Eswaran et al. (1993) respectively, but Batjes (1996) gives approximately 2400 Gt C. The six DGVMs compared by Cramer et al. (2001) all simulate lower values, in the range 850–

1200 Gt C. Considering these uncertainties, we may only say that the LPJmL total soil carbon and its depletion due to land use change are plausible.

Harvested carbon

Compared against statistics derived from FAO data for the year 2000 (K.H. Erb & F. Kraussmann, personal communication) our global simulation of total crop and grazing harvest appears too high, especially for grazing (Fig. 15d). Wirsenius (2003) estimated the global appropriation of terrestrial phytomass production by the food system to be around $5.9 \, \text{Pg C yr}^{-1}$ for the early 1990s. This number includes removed by-products such as straw, while we get a similar value without residues (Fig. 15e lower curve). The main problem seems to be grazing which LPJmL simulates with rather high intensity everywhere. Results are expected to improve when livestock density, as well as the impact of soil degradation on NPP are accounted for (reduction in extensively used or overgrazed areas).

Carbon fluxes

Previous studies using LPJ show natural vegetation to be a net carbon sink in the second half of the 20th century (Cramer *et al.*, 2001; Sitch *et al.*, 2003; Schaphoff *et al.*, 2006). McGuire *et al.* (2001), using a very simple representation of the effects of land use change on the carbon cycle within LPJ, broadly showed a picture similar to LPJmL: a net source until 1970, then a small sink. LPJmL simulated values of $0.04–0.16 \, \text{Pg C yr}^{-1}$ for the 1980s and $-0.61 – -0.75 \, \text{Pg C yr}^{-1}$ for the 1990s that fit within the range of recent estimates (1980s/1990s): $-0.2 \pm 0.7 / -1.4 \pm 0.7 \, \text{Pg C yr}^{-1}$ (Schimel *et al.*, 2001), $-0.3 \pm 0.9 / -1.2 \pm 0.9 \, \text{Pg C yr}^{-1}$ (Bopp *et al.*, 2002) and $-0.4 \pm 0.7 / -0.7 \pm 0.8 \, \text{Pg C yr}^{-1}$ (Plattner *et al.*, 2002).

Emissions due to land-use change until 1970 are simulated by LPJmL to be in good agreement with Houghton (2003). Despite the fact that different land use data generate twofold changes in simulated emissions for the following decades, the LPJmL simulations remain within the range from other studies: $0.6–2.5 \, \text{Pg C yr}^{-1}$ (1980s, Schimel *et al.*, 2001) and $0.8–2.4 \, \text{Pg C yr}^{-1}$ (1990s, Schimel *et al.*, 2001), and $1.4–3 \, \text{Pg C yr}^{-1}$ (1990s, House *et al.*, 2003). The large uncertainty expressed by the estimates of recent deforestation rates and the size of the terrestrial carbon sink demonstrates the large degree of uncertainty present in current data and interpretation. Results from process-based models such as LPJmL do not necessarily reduce this uncertainty, but they offer insights into the potential causes of the biogeochemical fluxes and their future development.

Sowing date

Broadly, the simulated sowing dates, and the selection of summer and winter types in cereals compare well with observations, although the USDA country-level sowing dates for temperate cereals allow only a qualitative comparison (Fig. 4). Better tests require gridded observations rather than country data. Regional data from a combination of local statistics and expert knowledge are now being assembled for many countries (e.g. Kucera & Genovese, 2004), and satellite derived data may also become available (e.g. Liew *et al.*, 1998). To assess how simulated 20th century trends in sowing date simulation are realistic is also difficult, as farming practices, machine technology and cultivar availability all play major roles.

Crop yield

Based on fertilizer use, we scaled a cultivation intensity related parameter (LAI_{max}) between countries. This produced realistic LPJmL yield simulations for the present (Figs 8 and 10). However, we do not consider technological or management changes over time (except irrigation) and, therefore, overestimate simulated yields in earlier decades of the 20th century (not shown), for a number of reasons. Most crops had much lower harvests around 1900, as the development toward high-yielding cultivars occurred mainly since 1960. Industrial fertilizers were broadly applied only after 1950 and their use has increased dramatically since. To account for such changes, the IMAGE team (2001) considers an empirical dynamic management factor that adjusts the simulated potential yields since 1970. Regional studies using detailed information about cultivars and farming practices are expected to provide more process-related model improvements for later generalization. In such a study with ORCHIDEE–STICS, Gervois (2004) was able to reproduce the 20th century observed yield trend for wheat in France. Additional investigations are needed to represent such temporal changes at the global scale in LPJmL.

While the global rate of increase of crop yields appears to be declining (Wollenweber *et al.*, 2005), predictions of future trends in farming practices, plant breeding, development of genetically modified organisms, are all uncertain. Overall, global fertilizer use will increase substantially, but its rate and geographic distribution may change due to environmental concerns, differences in socioeconomic conditions, and technological as well as political factors. Analysing several economic scenarios in Europe for the 21st century, Ewert *et al.* (2005) illustrated the importance of technology development for crop productivity. LPJmL is struc-

turally equipped to test hypotheses for the impact of such developments in the future, as long as the relevant information to parameterize these adequately is available.

Seasonal carbon fluxes

Monthly CO_2 fluxes simulated by LPJmL for specific crops compared well with observations from three sites (Fig. 11). For a more quantitative comparison against measured fluxes, LPJmL will have to be constrained with local information on the farming practices, as well as a better soil type characterization, and then run with daily meteorological data from the site. Additional tests are planned for a greater number of crop sites now becoming available, (e.g. from CarboEurope-IP; http://www.carboeurope.org).

Land use data

The reconstruction of the distribution of rain-fed and irrigated CFTs during the 20th century suffers from several shortcomings. Inevitably, different published data sets have some inconsistencies, (e.g. some grid cells which were reported as being more than 70% equipped for irrigation in the 1990s; Döll & Siebert, 1999) had no cropland areas according to Ramankutty & Foley (1999). A number of such data problems are being addressed now (e.g. Ramankutty, 2004). Another problem is due to our assumption that the relative crop distribution within a grid cell remains constant during the 20th century. In reality, socioeconomic and political factors determining land allocation have changed in many areas. Soybean, for example, was still marginal in Argentina in the early 1960s and it is now grown on a larger area than wheat (FAOSTAT, 2004). The differentiation between wheat and soybean croplands may have little relevance for the first order estimation of GHG emissions due land use change, but it becomes important when their respective growing seasons and managements impact differently on biogeochemical fluxes, soil carbon and on climate. When crop production is simulated for food/feed or bioenergy assessments then this differentiation becomes imperative.

Some particular problems occur: for maize, the map of Leff et al. (2004) does not distinguish grain maize from fodder maize. Currently, the maize CFT in LPJmL corresponds to grain maize, which achieves rather low yields in northern areas (Fig. 9). Since in much of this area in reality fodder maize is grown (and as good spatial data for its distribution is missing), this underestimation of yield is difficult to overcome. In the absence of reliable data, we also assume that only rice was irrigated in 1900, but this is clearly not the case for

countries like Egypt where irrigation has occurred for several millennia, and was already expanded during the 19th century.

Better data are required for grassland, as we were not aware of a published global data set providing the cover fraction of managed grassland. Further, carbon dynamics under cutting or grazing management differ (Orr et al., 1988). Many studies also showed that grazing intensity impacts soil carbon (e.g. Frank et al., 1995). Therefore, the implementation of a better parameterization for cutting/grazing within LPJmL will require the use of available data sets on grassland managements, like maps on livestock distribution (Kruska et al., 2003).

CFT diversity

The current list of CFTs in LPJmL represents an attempt to cover the world's major crops, but it could be expanded or reduced for different purposes. Simulating all CFTs indicated by the present land use data set is computationally expensive. Global comparisons (not shown here) show that comparable results can be achieved for global stocks and fluxes when only the three most important CFTs in each grid cell are considered. A trade-off exists between the availability of historical information about the distribution of crops and the need to differentiate between them. For example, sunflower, soybean, groundnuts and rapeseed all belong to 'oil crops' in the HYDE land use database (Klein Goldewijk & Battjes, 1997), but their biogeochemical functions differ substantially (e.g. the groundnuts cycle depends on precipitation, while winter rapeseed has vernalization requirements). We, therefore, assign different CFTs to them. For assessments of food production, additional diversity is required, [e.g. to distinguish between potatoes and sugar beets (currently both in 'temperate roots')].

Water use

It is possible to use LPJmL for estimation of spatial and temporal changes in crop water use in response to changing CO_2 and climate. This is important as the predicted increasing demand in land for food, feed and bioenergy is expected to face water scarcity problems (Postel, 1998). A river routine module is currently implemented in a future model version, and this will limit the amount of water available for irrigation. For water supply from other sources (fossil groundwater resources or reservoirs) no appropriate data could be identified.

GHG fluxes, soil fertility

The current version of LPJmL simulates only CO_2 fluxes – other GHG fluxes will be implemented into the same structure, beginning with emissions of methane from rice paddies and grazing animals, and N_2O emissions. This is required for the assessment of various policies (limitation of fertilizer use, temporary drainage of flooded rice fields for methane emission mitigation, e.g. Li *et al.*, 2005), and is linked to the representation of nutrient limitation in LPJmL. Soil organic matter, soil fertility and carbon emission are also related to the processing of residues, like tillage (Holland & Coleman, 1987), or straw burning, either in the fields or used as biofuel (Yevich & Logan, 2003). In order to test the impact of different management practices (related to specific agricultural systems or environmental policies) on soil conservation and GHG emissions, better management data are required at the global scale (Heistermann *et al.*, 2006), but work is underway to improve the situation (e.g. Bouwman *et al.*, 2005).

Future land use

The present study uses input data that prescribe historical land use, but for scenario calculations land use should be a dynamic variable. Land allocation is determined by potential crop productivity, and by socio-economic and political factors including commodity markets, technology and capital. As a first step, LPJmL can replace crop suitability concepts such as the Agro Ecological Zones (AEZ) model (Fischer *et al.*, 2002) to determine shifts in the most appropriate areas for the cultivation of major crops due to changes in climate. It is also possible to consider the yield level simulated by LPJmL in an economic land use model that estimates the land use shares at the grid-cell level and returns this information to LPJmL for a consistent assessment of the biogeochemical cycles. The results from a prototype version of such a land use model are shown for Germany by Lotze-Campen *et al.* (2005).

Conclusion

The LPJmL modelling strategy is simple enough to allow for global assessments of agricultural impacts on the terrestrial biogeochemical cycles, across multiple decades, and for the majority of crop types worldwide. Using an earlier LPJ version and a crude representation of croplands, McGuire *et al.* (2001), already showed the significance of land use for the terrestrial carbon cycle. By implementing a process-based representation of crops growth and harvesting fully consistent with LPJ, we account for most of the interactions between CO_2, climate, and land use to represent spatial and temporal dynamics of important biophysical and biogeochemical parameters, including the simulation of crop productivity. Unlike very detailed crop models requiring many input parameters, LPJmL simulates significant parameters of the crop phenology directly on the basis of the local climate, making the model widely applicable.

The benchmarking exercises have demonstrated the validity of the concept. We could quantify the role of land use on water and carbon cycles during the 20th century, including a global estimation of carbon harvested for food. LPJmL can, therefore, be used to test the impact of different management or land use scenarios on the biogeochemical cycles as related to food/feed production (Müller *et al.*, 2006). Even if predictions of technology changes are very uncertain, it is expected that LPJmL performs credibly under conditions that do not exist today, such as under higher atmospheric [CO_2], to assess the future role of land use within the climate-vegetation system (Zaehle *et al.*, in press; Schröter *et al.*, 2005; Müller *et al.*, manuscript).

References

Alcamo J, Van Vuuren D, Ringler C *et al.* (2005) Changes in nature's balance sheet: model-based estimates of future worldwide ecosystem services. *Ecology and Society*, **10**, 19 [online] URL: http://www.ecologyandsociety.org/vol10/iss2/art19/

Arnold JG, Williams JR, Srinivasan R *et al.* (1994) *SWAT, soil and water assessment tool*. Report, USDA, Agriculture Research Service, Grassland, Soil & Water Research Laboratory, Temple, TX, US.

Avissar R, Werth D (2005) Global hydroclimatological teleconnections resulting from tropical deforestation. *Journal of Hydrometeorology*, **6**, 134–145.

Batjes NH (1996) Total carbon and nitrogen in the soils of the world. *European Journal of Soil Science*, **47**, 151–163.

Betts RA (2001) Biogeophysical impacts of land use on present-day climate: near-surface temperature and radiative forcing. *Atmospheric Science Letters*, **2**, 39–51.

Bonan GB (1999) Frost followed the plow: impacts of deforestation on the climate of the United States. *Ecological Applications*, **9**, 1305–1315.

Bopp L, Le Quéré C, Heimann M et al. (2002) Climate-induced oceanic oxygen fluxes: implications for the contemporary carbon budget. *Global Biogeochemical Cycles*, **16**, 1022, doi: 10.1029/2001GB001445.

Boswell VG (1926) The influence of temperature upon the growth and yield of garden peas. *Proceedings of the American Society for Horticultural Sciences*, **23**, 162–168.

Boucher O, Myhre G, Myhre A (2004) Direct human influence of irrigation on atmospheric water vapour and climate. *Climate Dynamics*, **22**, 597–603.

Bouwman AF, Van Der Hoek KW, Eickhout B et al. (2005) Exploring changes in world ruminant production systems. *Agricultural Systems*, **84**, 121–153.

Bradford JB, Lauenroth WK, Burke IC (2005) The impact of cropping on primary production in the U.S. Great Plains. *Ecology*, **86**, 1863–1872.

Brisson N, Gary C, Justes E et al. (2003) An overview of the crop model STICS. *European Journal of Agronomy*, **18**, 309–332.

Brovkin V, Claussen M, Driesschaert E (2006) Biogeophysical effects of historical land cover changes simulated by six Earth system models of intermediate complexity. *Climate Dynamics*, **26**, 587–600.

Brovkin V, Sitch S, von Bloh W et al. (2004) Role of land cover changes for atmospheric CO_2 increase and climate change during the last 150 years. *Global Change Biology*, **10**, 1–14.

Caviness CE, Collins FC, Sullivan M (1986) Effect of wheat residue on early growth of soybean. *Arkansas Farm Research*, **35**, 8.

Challinor AJ, Slingo JM, Wheeler TR et al. (2004) Design and optimisation of a large-area process-based model for annual crops. *Agricultural and Forest Meteorology*, **124**, 99–120.

Challinor AJ, Wheeler TR, Osborne TM et al. (2006) Assessing the vulnerability of crop productivity to climate change thresholds using an integrated crop-climate model. In: *Avoiding Dangerous Climate Change* (eds Schellnhuber H-J, Cramer W, Nakicenovic N, Wigley T, Yohe G), pp. 187–194. Cambridge University Press, Cambridge, UK.

Cramer W, Bondeau A, Schaphoff S et al. (2004) Tropical forests and the global carbon cycle: impacts of atmospheric carbon dioxide, climate change and rate of deforestation. *Philosophical Transactions of the Royal Society London, Series B*, **359**, 331–343.

Cramer W, Bondeau A, Woodward FI et al. (2001) Global response of terrestrial ecosystem structure and function to CO_2 and climate change: results from six dynamic global vegetation models. *Global Change Biology*, **7**, 357–373.

DeFries RS, Field CB, Fung I et al. (1999) Combining satellite data and biogeochemical models to estimate global effects of human-induced land cover change on carbon emissions and primary productivity. *Global Biogeochemical Cycles*, **13**, 803–815.

de Noblet-Ducoudré N, Claussen M, Prentice IC (2000) Mid-Holocene greening of the Sahara: comparing the response of two coupled atmosphere/biome models. *Climate Dynamics*, **16**, 643–659.

de Noblet-Ducoudré N, Gervois S, Ciais P et al. (2004) Coupling the Soil-Vegetation-Atmosphere-Transfer Scheme ORCHIDEE to the agronomy model STICS to study the influence of croplands on the European carbon and water budgets. *Agronomie*, **24**, 1–11.

Döll P, Siebert S (1999) *A Digital Global Map Of Irrigated Areas – Documentation*. University of Kassel, Kassel.

Donner SD, Kucharik CJ (2003) Evaluating the impacts of land management and climate variability on crop production and nitrate export across the Upper Mississippi Basin. *Global Biogeochemical Cycles*, **17**, 1085, doi: 10.1029/2001GB001808.

Eswaran H, Van den Berg E, Reich P (1993) Organic carbon in soils of the World. *Soil Science Society of America Journal*, **57**, 192–194.

Evans LT (1997) Adapting and improving crops: the endless task. *Philosophical Transactions of the Royal Society London, Series B*, **352**, 901–906.

Ewert F, Metzger MJ, Rounsevell MDA et al. (2005) Future scenarios of European agricultural land use. I: estimating changes in crop productivity. *Agriculture, Ecosystems and Environment*, **107**, 101–116.

FAO (1978) *Report on the Agro-Ecological-Zones Project, Vol. 1: Methodology and Results for Africa*. FAO, Rome.

FAOSTAT data (2004), http://faostat.fao.org/ [Accessed: May, 2004].

Farquhar GD, von Caemmerer S, Berry JA (1980) A biochemical model of photosynthetic CO_2 assimilation in leaves of C_3 species. *Planta*, **149**, 78–90.

Feddema JJ, Oleson KW, Bonan GB et al. (2005) A comparison of a GCM response to historical anthropogenic land cover change and model sensitivity to uncertainty in present-day land cover representations. *Climate Dynamics*, **25**, 581–609.

Fernandez-Rivera S, Lewis M, Klopfenstein TJ et al. (1989) A simulation model of forage yield, quality and intake and growth of growing cattle grazing cornstalks. *Journal of Animal Science*, **67**, 581–589.

Fischer G, Shah M, van Velthuizen H et al. (2002) *Global Agro-Ecological Assessment for Agriculture in the 21st Century: Methodology and results*. IIASA Research Report RR-02-02, Laxenburg, Austria.

Foley JA, DeFries RS, Asner GP et al. (2005) Global consequences of land use. *Science*, **309**, 570–574.

Foley JA, Prentice IC, Ramankutty N et al. (1996) An integrated biosphere model of land surface processes, terrestrial carbon balance, and vegetation dynamics. *Global Biogeochemical Cycles*, **10**, 603–628.

Frank AB, Tanaka DL, Hofmann L et al. (1995) Soil carbon and nitrogen of Northern Great Plains grasslands as influenced by long-term grazing. *Journal of Range Management*, **48**, 470–474.

Fujisaka S, Harrington L, Hobbs P (1994) Rice-wheat in South Asia: systems and long-term priorities established through diagnostic research. *Agricultural Systems*, **46**, 169–187.

Gerten D, Bondeau A, Hoff H et al. (2004a) Assessment of 'green' water fluxes with a dynamic global vegetation model. In:

Hydrology: Science & Practice for the 21st Century (eds Webb B, Arnell N, Onofet C), British Hydrological Society, 1, 29–35.

Gerten D, Schaphoff S, Haberlandt U *et al.* (2004b) Terrestrial vegetation and water balance – hydrological evaluation of a dynamic global vegetation model. *Journal of Hydrology*, 286, 249–270.

Gervois S (2004) *Les zones agricoles en Europe: évaluation de leur rôle sur les bilans d'eau et de carbone à l'échelle de l'Europe; sensibilité de ces bilans aux changements environnementaux sur le vingtième siècle.* Ph.D. Thesis, University Paris VI. 209 pp (in French).

Gervois S, de Noblet-Ducoudré N, Viovy N *et al.* (2004) Including croplands in a global biosphere model: methodology and evaluation at specific sites. *Earth Interactions*, 8, 1–25.

Gordon LJ, Steffen W, Jönsson BF *et al.* (2005) Human modification of global water vapor flows from the land surface. *Proceedings of the National Academy of Sciences of the United States of America*, 102, 7612–7617.

Guo LB, Gifford RM (2002) Soil carbon stocks and land use change: a meta analysis. *Global Change Biology*, 8, 345–360.

Harrison PA, Downing TE, Porter JR (2000) Scaling-up the AFRCWHEAT2 model to assess phenological development for wheat in Europe. *Agricultural and Forest Meteorology*, 101, 167–186.

Haxeltine A, Prentice IC (1996) BIOME3: an equilibrium terrestrial model based on ecophysiological constraints, resource availability and competition among plant functional types. *Global Biogeochemical Cycles*, 10, 693–709.

Heistermann M, Müller C, Ronneberger K (2006) Land in sight? Achievements, deficits and potentials of continental to global scale land-use modeling. *Agriculture, Ecosystems and Environment*, 114, 141–158.

Holland EA, Coleman DC (1987) Litter placement effects on microbial and organic matter dynamics in an agroecosystem. *Ecology*, 68, 425–433.

Houghton RA (2003) Revised estimates of the annual net flux of carbon to the atmosphere from changes in land use and land management 1850–2000. *Tellus Series B, Chemical and Physical Meteorology*, 55, 378–390.

House JI, Prentice IC, Ramankutty N *et al.* (2003) Reconciling apparent inconsistencies in estimates of terrestrial CO_2 sources and sinks. *Tellus Series B, Chemical and Physical Meteorology*, 55, 345–363.

IFA (2002) *Fertilizer Use by Crop*, 5th edn; http://www.fertilizer.org/ifa/statistics.asp. Rome, International Fertilizer Industry Association.

IMAGE team (2001) *The IMAGE 2.2 Implementation of the SRES Scenarios: A Comprehensive Analysis of Emissions, Climate Change and Impacts in the 21st century.* National Institute for Public Health and the Environment, RIVM, Bilthoven, the Netherlands, CD-ROM publication 481508018.

King JA, Harrison R, Carter AD *et al.* (2004) Carbon sequestration and saving potential associated with changes to the management of agricultural soils in England. *Soil Use and Management*, 20, 394–402.

Klein Goldewijk K, Battjes JJ (1997) *A hundred Year (1890–1990) Database for Integrated Environmental Assessments (HYDE, version 1.1).* National Institute of Public Health and the Environment (RIVM), Bilthoven, the Netherlands.

Krinner G, Viovy N, de Noblet-Ducoudré N *et al.* (2005) A dynamic global vegetation model for studies of the coupled atmosphere-biosphere system. *Global Biogeochemical Cycles*, 19, GB1015, doi: 10.1029/2003GB002199.

Kruska RL, Reid RS, Thornton PK *et al.* (2003) Mapping livestock-oriented agricultural production systems for the developing world. *Agricultural Systems*, 77, 39–63.

Krysanova V, Hattermann F, Wechsung F (2005) Development of the ecohydrological model SWIM for regional impact studies and vulnerability assessment. *Hydrological Processes*, 19, 763–783.

Krysanova V, Wechsung F, Arnold J *et al.* (2000) *SWIM (soil and water integrated model). User manual.* PIK Report 69, Potsdam-Institut für Klimafolgenforschung, Potsdam, Germany.

Kucera L, Genovese G (2004) Crop monographies on central European countries – MOCA Study, Joint Research Centre, Ispra, Italy. http://agrifish.jrc.it/marsstat/Crop_Yield_Forecasting/MOCA/

Kucharik CJ (2003) Evaluation of a process-based agro-ecosystem model (Agro-IBIS) across the US corn belt: simulations of the interannual variability in maize yield. *Earth Interactions*, 7, 1–33.

Kucharik CJ, Brye KR (2003) Integrated biosphere simulator (IBIS) yield and nitrate loss predictions for Wisconsin maize receiving varied amounts of nitrogen fertilizer. *Journal of Environmental Quality*, 32, 247–268.

Lal R (2005) World crop residues production and implications of its use as a biofuel. *Environment International*, 31, 575–584.

Leahy P, Kiely G, Scanlon TM (2004) Managed grasslands: a greenhouse gas sink or source? *Geophysical Research Letters*, 31, 20.

Leff B, Ramankutty N, Foley JA (2004) Geographic distribution of major crops across the world. *Global Biogeochemical Cycles*, 18, GB1009, doi: 10.1029/2003GB002108.

Levy PE, Friend AD, White A *et al.* (2004) The influence of land use change on global-scale fluxes of carbon from terrestrial ecosystems. *Climatic Change*, 67, 185–209.

Li C, Frolking S, Xiao X *et al.* (2005) Modelling impacts of farming management alternatives on CO_2, CH_4 and N_2O emissions: a case study for water management of rice agriculture of China. *Global Biogeochemical Cycles*, 19, GB3010, doi: 10.1029/2004GB002341.

Liew SC, Kam SP, Tuong TP *et al.* (1998) Application of multitemporal ERS-2 synthetic aperture radar in delineating rice cropping systems in the Mekong River Delta, Vietnam. *IEEE Transactions on Geoscience and Remote Sensing*, 36, 1412–1420.

Lohila A, Aurela M, Tuovinen J-P *et al.* (2004) Annual CO_2 exchange of a peat field growing spring barley or perennial forage grass. *Journal of Geophysical Research D: Atmospheres*, 109, D18116, doi: 10.1029/2004JD004715.

Lopez-Guisa JM, Satter LD, Panciera M (1991) Utilization of ensiled corn crop residues by Holstein heifers. *Journal of Dairy Science*, 74, 3160–3166.

Lotze-Campen H, Müller C, Bondeau A *et al.* (2005) How tight are the limits to land and water use? – Combined impacts of food demand and climate change. *Advances in Geosciences*, 4, 23–28.

Lucht W, Prentice IC, Myneni RB et al. (2002) Climatic control of the high-latitude vegetation greening trend and Pinatubo effect. Science, 296, 1687–1689.

McGuire A, Sitch S, Clein J et al. (2001) Carbon balance of the terrestrial biosphere in the twentieth century: analyses of CO_2, climate and land use effects with four process-based ecosystem models. Global Biogeochemical Cycles, 15, 183–206.

Meireles EJL, Pereira AR, Sentelhas PC et al. (2002) Calibration and test of the cropgro-dry bean model for edaphoclimatic conditions in the savanas of central Brazil. Scienta Agricola, 59, 723–729.

Monsi M, Saeki T (1953) Über den Lichtfaktor in den Pflanzen-gesellschaften und seine Bedeutung für die Stoffproduktion. Japanese Journal of Botany, 14, 22–52.

Monteith JL (1972) Solar radiation and productivity in tropical ecosystems. Journal of Applied Ecology, 9, 747–766.

Müller C, Bondeau A, Lotze-Campen H et al. (2006) Comparative impact of climatic and non-climatic factors on global terrestrial carbon and water cycles. Global Biogeochemical Cycles, 20, GB4015, doi: 10.1029/2006GB002742.

Müller C, Eickhout B, Zaehle S et al. (manuscript). Effects of changes in CO_2, climate and land-use on the carbon balance of the land biosphere during the 21st century.

Myneni RB, Nemani RR, Running SW (1997) Estimation of global leaf area index and absorbed PAR using radiative transfer models. IEEE Transactions on Geoscience and Remote Sensing, 35, 1380–1393.

Neitsch SL, Arnold JG, Kiniry JR et al. (2002) Soil and Water Assessment Tool. Theoretical Documentation + User's Manual. USDA-ARS-SR Grassland, Soil and Water Research Laboratory. Agricultural Research Service, Temple, TX, US.

New M, Hulme M, Jones P (2000) Representing twentieth century space-time climate variability. II: development of 1901–1996 monthly grids of terrestrial surface climate. Journal of Climate, 13, 2217–2238.

Österle H, Gerstengarbe FW, Werner PC (2003) Homogenisierung und Aktualisierung des Klimadatensatzes des Climate Research Unit der Universität of East Anglia, Norwich. Terra Nostra, 6. Deutsche Klimatagung 2003, Potsdam, Germany (in German).

Ogle SM, Paustian K, Breidt FJ (2005) Agricultural management impacts on soil organic carbon storage under moist and dry climatic conditions of temperate and tropical regions. Biogeochemistry, 72, 87–121.

Olson J, Watts JA, Allison LJ (1985) Major World Ecosystem Complexes Ranked by Carbon in Live Vegetation: A Database. Carbon Dioxide Information Center, Oak Ridge National Laboratory, Oak Ridge, TN.

Orr RJ, Parsons AJ, Treacher TT et al. (1988) Seasonal patterns of grass production under cutting or continuous stocking man-agements. Grass and Forage Science, 43, 199–207.

Parton WJ, Hartman MD, Ojima DS et al. (1998) DAYCENT and its land surface submodel: description and testing. Global and Planetary Change, 19, 35–48.

Peylin P, Bousquet P, Le Quéré C et al. (2005) Multiple constraints on regional CO_2 flux variations over land and oceans. Global Biogeochemical Cycles, 19, GB1011, doi: 10.1029/2003GB002214.

Plattner G-K, Joos F, Stocker TF (2002) Revision of the global carbon budget due to changing air-sea oxygen fluxes. Global Biogeochemical Cycles, 16, 1096, doi: 10.1029/2001GB001746.

Post WM, Emanuel WR, Zinke PJ (1982) Soil carbon pools and world life zones. Nature, 298, 156–159.

Postel SL (1998) Water for food production: will there be enough in 2025? BioScience, 48, 629–637.

Powell JM, Pearson RA, Hiernaux PH (2004) Crop-livestock interactions in the West African drylands. Agronomy Journal, 96, 469–483.

Prentice IC, Bondeau A, Cramer W et al. (2006) Dynamic global vegetation modelling: quantifying terrestrial ecosystem re-sponses to large-scale environmental change. In: Terrestrial Ecosystems in a Changing World (eds Canadell JG, Pataki D, Pitelka LF), pp. 175–192. Springer-Verlag, Berlin.

Prentice IC, Heimann M, Sitch S (2000) The carbon balance of the terrestrial biosphere: ecosystem models and atmospheric ob-servations. Ecological Applications, 10, 1553–1573.

Ramankutty N (2004) Croplands in West Africa: a geographically explicit dataset for use in models. Earth Interactions, 8, 1–22.

Ramankutty N, Foley JA (1999) Estimating historical changes in global land cover; croplands from 1700 to 1992. Global Biogeo-chemical Cycles, 13, 997–1028.

Reichstein M, Falge E, Baldocchi D et al. (2005) On the separation of net ecosystem exchange into assimilation and ecosystem respiration: review and improved algorithm. Global Change Biology, 11, 1424–1439.

Saugier B, Roy J, Mooney HA (2001) Estimations of global terrestrial productivity: converging toward a single number? In: Terrestrial Global Productivity (eds Roy J, Saugier B, Mooney HA), pp. 543–557. Academic Press, San Diego.

Schaphoff S, Lucht W, Gerten D et al. (2006) Terrestrial biosphere carbon storage under alternative climate projections. Climatic Change, 74, 97–122.

Schimel DS, House JI, Hibbard KA et al. (2001) Recent patterns and mechanisms of carbon exchange by terrestrial ecosystems. Nature, 414, 169–172.

Schröter D, Cramer W, Leemans R et al. (2005) Ecosystem service supply and vulnerability to global change in Europe. Science, 310, 1333–1337.

Sheehan J, Aden A, Paustian K et al. (2004) Energy and environ-mental aspects of using corn stover for fuel ethanol. Journal of Industrial Ecology, 7, 117–146.

Sitch S, Smith B, Prentice IC et al. (2003) Evaluation of ecosystem dynamics, plant geography and terrestrial carbon cycling in the LPJ dynamic global vegetation model. Global Change Biology, 9, 161–185.

Stehfest E, Heistermann M, Priess JA et al. (manuscript in preparation) Simulation of global crop production with the Ecosystem model DayCent.

Stockle CO, Williams JR, Rosenberg NJ et al. (1992) A method for estimating the direct and climatic effects of rising atmospheric carbon dioxide on growth and yield of crops: part 1 – Mod-ification of the EPIC model for climatic change analysis. Agricultural Systems, 38, 225–238.

Tan G, Shibasaki R (2003) Global estimation of crop productivity and the impacts of global warming by GIS and EPIC integra-tion. Ecological Modelling, 168, 357–370.

USDA (1994) Major world crop areas and climatic profiles. *Agricultural Handbook 664, US Department of Agriculture (USDA)*, World Agricultural Outlook Board, Joint Agricultural Weather Facility Washington, DC.

Wagner W, Scipal K, Pathe C *et al.* (2003) Evaluation of the agreement between the first global remotely sensed soil moisture data with model and precipitation data. *Journal of Geophysical Research*, **108**, 4611, doi: 10.1029/2003JD003663.

WBGU (1998) *The accounting of biological sinks and sources under the kyoto protocol – a step forwards or backwards for global environmental protection?* WBGU Special Report, Bremerhaven, Germany, 75 pp.

Weir AH, Bragg PL, Porter JR *et al.* (1984) A winter wheat crop simulation model without water or nutrient limitations. *Journal of Agricultural Science*, **102**, 371–382.

Wilhelm WW, Johnson JMF, Voorhees WB *et al.* (2004) Crop and soil productivity response to corn residue removal: a literature review. *Agronomy Journal*, **96**, 1–17.

Williams JR, Jones CA, Kiniry JR *et al.* (1989) The EPIC crop growth model. *Transactions of the American Society of Agricultural Engineers*, **32**, 497–511.

Wirsenius S (2003) The biomass metabolism of the food system, a model-based survey of the global and regional turnover of food biomass. *Journal of Industrial Ecology*, **7**, 47–80.

Wollenweber B, Lübberstedt T, Porter JR (2005) Need for multi-disciplinary research towards a second green revolution. *Current Opinion in Plant Biology*, **8**, 337–341.

Xue Y (1996) The impact of desertification in the Mongolian and the Inner Mongolian grassland on the regional climate. *Journal of Climate*, **9**, 2173–2189.

Yadvinder-Singh B-S, Ladha JK, Khind CS *et al.* (2004) Effects of residue decomposition on productivity and soil fertility in rice–wheat rotation. *Soil Science Society of America Journal*, **68**, 854–864.

Yevich R, Logan JA (2003) An assessment of biofuel use and burning of agricultural waste in the developing world. *Global Biogeochemical Cycles*, **17**, 6–1.

Zaehle S (2005) *Process-based simulation of the European terrestrial biosphere – An evaluation of present-day and future terrestrial carbon balance estimates and their uncertainty.* PhD thesis. Universität Potsdam. Potsdam, Germany.

Zaehle S, Bondeau A, Cramer W *et al.* (in press) Projected changes in terrestrial carbon storage in Europe under climate and land-use change, 1990–2100.

Zaehle S, Sitch S, Smith B *et al.* (2005) Effects of parameter uncertainties on the modeling of terrestrial biosphere dynamics. *Global Biogeochemical Cycles*, **19**, GB3020, doi: 10.1029/2004GB002395.